Physicochemical and urban land-use characteristics associated with resistance to precipitation in estuaries vary across scales

Anna B. Turetcaia[1,*], Nicole G. Dix[2], Hannah Ramage[3], Matthew C. Ferner[4], Emily B. Graham[1,5,*]

[1] Pacific Northwest National Laboratory, Richland, WA 99352, USA
[2] Guana Tolomato Matanzas National Estuarine Research Reserve, Ponte Vedra Beach, FL 32082, USA
[3]Lake Superior National Estuarine Research Reserve, University of Wisconsin Madison, Division of Extension, Superior, WI 54880, USA
[4] San Francisco State University, Estuary and Ocean Science Center, Tiburon, CA 94920, USA
[5] School of Biological Sciences, Washington State University, Pullman, WA 99164, USA

Correspondence to: Anna B. Tureţcaia (anna.turetcaia@pnnl.gov) and Emily B. Graham (emily.graham@pnnl.gov)

Abstract. Estuaries are subject to frequent stressors, including elevated nutrient loading and extreme hydrologic events, which impact water quality and disrupt ecosystem stability and health. The capacity of an estuary to resist changes in function in response to precipitation events is a key component of maintaining estuarine health in our changing climate. However, generalizable patterns in factors related to estuarine responses to extreme precipitation remain unknown. We investigate physicochemical factors and land-use characteristics that are associated with ecological resistance to precipitation – broadly defined as the magnitude of ecosystem change induced by an event – in five disparate estuaries distributed across the continental United States. Using long-term meteorological and water quality data from the National Estuarine Research Reserve System along with land use/land cover and population data, we examine relationships between the resistance index – a proxy for ecosystem stability calculated using dissolved oxygen – and physicochemical and urban land use characteristics on local-to-continental scales. Contrary to our initial hypothesis, we found that more urbanized estuaries were more resistant to precipitation events, and that water temperature, water column depth, turbidity, nitrogen, and chlorophyll-*a* were related to resistance on a continental scale. However, these trends interacted with estuarine salinity and varied across individual estuaries; where we found additional relationships of resistance with salinity, turbidity, phosphate concentrations, N:P, and tree cover. Considering emerging stressors from new climatic scenarios and from urbanization, these results are important for representing the impacts of disturbances in large-scale models and for informing management decisions regarding estuarine water quality.

1. Introduction

Estuaries are highly dynamic environments that often connect freshwater and saltwater systems, cycle organic matter and nutrients from land to oceans, and provide essential ecosystem services (Bianchi, 2007; He and Silliman, 2019). The function of estuarine ecosystems as unique sites for carbon and nutrient cycling, and habitats for macro- and micro-flora and fauna, relies on stability of a predictable range of dynamic processes like temperature fluctuations, hydrology and nutrient mixing. However, anthropogenic activities and extreme climatic events threaten estuarine ecosystem stability and function (Kemp et al., 2009; Zhang et al., 2010). Predicted increases in urban population size and in the frequency and intensity of precipitation events highlight the urgency to understand the response of estuaries to new urban and climatic scenarios (Kyzar et al., 2021; Li et al., 2019; Martínez et al., 2007; Pickett et al., 2011). Yet, the factors that impact the response of urban estuaries to precipitation are not fully understood.

When combined with intense precipitation, watershed urbanization and associated changes in land use/land cover (LULC) often result in increases in stream hydrological flashiness (Gannon et al., 2022; Grimm et al., 2008; Reisinger et al., 2017). Hydrological flashiness induces increased flow rates that cause changes in channel morphology (Booth and Jackson, 1997; Gregory, 2011; Leopold, 1968; Vietz et al., 2016), habitat destruction (Walsh et al., 2005), and disruption of microbial metabolic processes (Reisinger et al., 2017; Uehlinger, 2000). Flashiness can also drastically affect primary production – a regulatory component of dissolved oxygen (DO) dynamics in aquatic environments – through increases in flow velocity, transport of phytoplankton, sediment migration, and light limitation through increased turbidity (Bernot et al., 2010; Fisher et al., 1982; McSweeney et al., 2017; Reisinger et al., 2017; Uehlinger, 2000).

While DO is dynamic and depends on a myriad of biological, chemical, and physical processes, it is essential for many estuarine functions and has been widely used as an indicator for overall ecosystem health (Abdul-Aziz et al., 2007; Abdul-Aziz and Gebreslase, 2023; Chapra, 2008; Cox, 2003; Kannel et al., 2007; Zhi et al., 2021). Dissolved oxygen is critical to maintaining the life cycles of macro- and micro-fauna, for example, and supports the biogeochemical cycling of carbon and nutrients by serving as a terminal electron acceptor (Bernhardt et al., 2018; Chapra, 2008; Zarnetske et al., 2012). Built areas in particular have been previously connected to altered aquatic DO concentrations and other water quality parameters (Bernhardt et al., 2008; Chang, 2005; Freeman et al., 2019; Vietz et al., 2016). Given the tight link between aquatic DO, land use, and diverse ecosystem functions, DO is an important indicator and holistic measure of estuarine health.

In addition to impacts on DO, extreme precipitation events are often associated with excess nitrogen (N) delivery and changes in salinity, particularly for waterways adjacent to urban-type LULC (Walsh et al., 2005). Nitrogen is central to mediating metabolic processes across a wide range of ecosystems and land covers (Mulholland et al., 2008; Schindler, 1977; Smith, 1984; Vitousek and Howarth, 1991). It is particularly important for primary production in aquatic ecosystems because many phytoplankton species are N-limited (Evans and Seemann, 1989; Howarth, 1988; Vitousek and Howarth, 1991). Further, extreme precipitation events are often associated with influx of freshwater (i.e., runoff) and/or saltwater (i.e., storm surges) into estuaries, which changes salinity, can induce stratification and hypoxia, and impact ecosystem metabolic functions (Rabalais et al., 2010; Wetz and Yoskowitz, 2013; Zhang et al., 2010). However, depending on the temporal and spatial scales of evaluation, the reported trends of estuarine responses to precipitation and salinity changes can be conflicting.

Commonalities in responses to major precipitation events across disparate estuaries can help to project long-term estuary health under progressive urbanization and more extreme climate events; but they have been difficult to decipher. This is, in part, due to variation in how the complex and interconnected dynamics within estuaries respond to precipitation, even at local scales. While Ombadi & Varadharajan (2022) report contrasting effects of urbanization on salinity during flood events when regional climate is considered, a continental-scale study by Kaushal et al. (2018) suggests that anthropogenic activity is associated with increasing salinity in waterways. However, the later study recognizes that regional, climatic, LULC, and geologic variabilities also influence salinization patterns. Similarly, continental-scale evaluations showed that waterways within small watersheds appear consistently less flashy than those in large watersheds; and that there is a substantial amount of variability in these relationships at regional scale (Baker et al., 2004; Gannon et al., 2022; Hopkins et al., 2015; Poff et al., 2006). Such variation in relationships across scales may be particularly prevalent in ecosystems influenced by anthropogenic activities (Hopkins et al., 2015; Poff et al., 2006), which demonstrates the importance of considering multiple spatial scales in understanding estuarine responses to changes in precipitation patterns and watershed land use.

We aim to uncover generalizable patterns of responses to large precipitation events across five estuaries spanning a gradient of urbanization and physicochemical properties. Using DO as an indicator of ecosystem health (Abdul-Aziz and Gebreslase, 2023), we evaluate estuary resistance to precipitation – defined here as the ability of estuaries to maintain stability in DO (Isbell et al., 2015; Lake, 2013; McCluney et al., 2014; Pimm, 1984; Utz et al., 2016; Van Meerbeek et al., 2021) – in the context of physicochemical factors and land-use characteristics at: 1) the continental-scale (i.e., across all estuaries); 2) across estuaries grouped by salinity; and 3) within each estuary. We hypothesize that urbanization decreases estuarine resistance to precipitation, and further that relationships of resistance with physicochemical and land-use factors will diverge with spatial scale and differences in ambient salinity. This study helps understanding how ongoing changes in climate and urbanization conditions influence estuarine ecosystem health.

2. Methods

2.1 Dataset description.

We used long-term water quality monitoring data from five estuaries in the National Estuarine Research Reserve System (NERRS, 2023) to understand factors associated with their resistance to precipitation events. Lake Superior (LKS), WI; Chesapeake Bay Maryland (CBM), MD (Jug Bay only); Guana Tolomato Matanzas (GTM), FL; Weeks Bay (WKB), AL; and San Francisco Bay (SFB), CA span climatic zones, land uses, and salinity (0.1–35 ppt) (Fig. 1, Table 1). Across all estuaries, there were a total of 19 monitoring locations (3 at CBM, and 4 at LKS, GTM, WKB, and SFB).

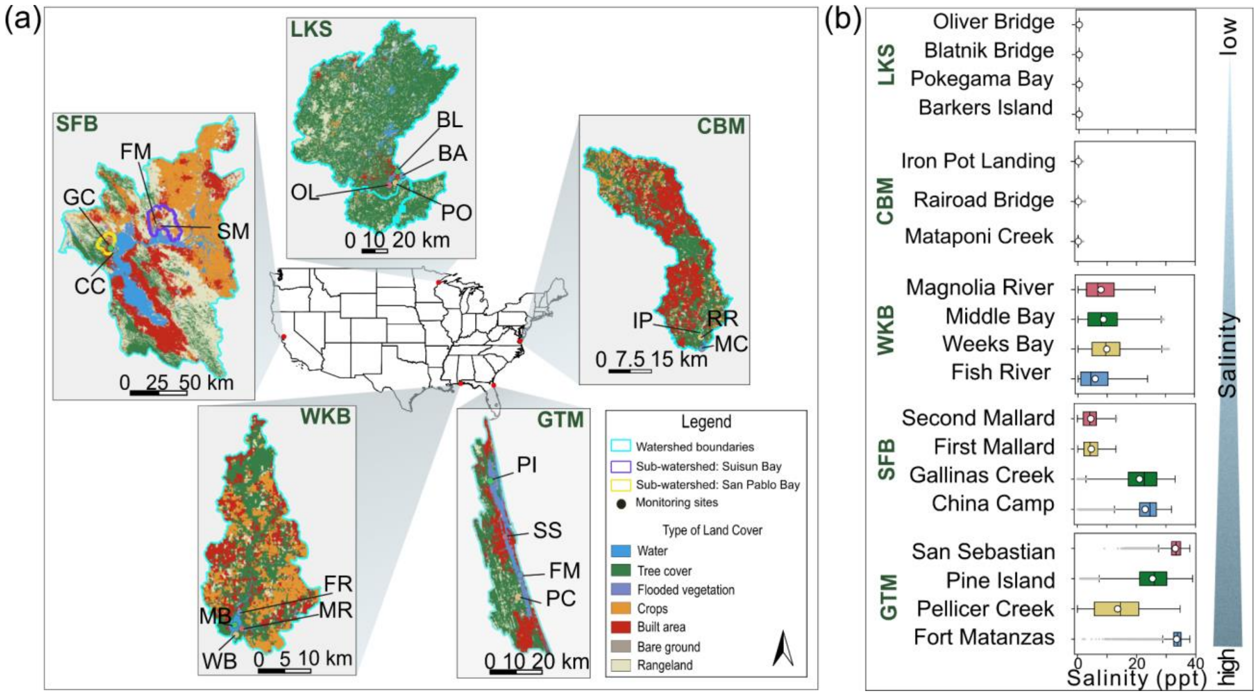

Figure 1. Selected National Estuarine Research Reserve (NERR) stations. a) Map of monitoring locations and land use/land cover within associated watersheds at Lake Superior (LKS) NERR, Chesapeake Bay, Maryland (CBM) NERR, Guana Tolomato Matanzas (GTM) NERR, Weeks Bay (WKB) NERR, and San Francisco Bay (SFB) NERR. b) Salinity from 2012 to 2022 for each monitoring location at each NERR (all n > 150,000). Boxes indicate interquartile range. Means are shown in white circles. Black lines inside the boxes indicate medians.

Table 1. Land use/land cover (LULC) and population density in each estuary within 10-km to water quality and nutrient monitoring locations.

LULC class	**Estuary and % LULC class within 10-km to monitoring locations**					
	LKS	*CBM (Jug Bay)*	*GTM*	*WKB*	*SFB*	
					(San Pablo Bay) CC, GC	*(Suisun Bay)* FM, SM
Water	10.43	2.30	8.58	4.85	5.04	3.59

Tree cover	58.78	53.72	45.11	38.52	26.91	1.16
Flooded vegetation	0.88	1.37	13.04	0.05	1.4	21.33
Crops	0.19	4.63	0.19	30.36	18.05	19.67
Built area	18.84	27.19	23.99	19.33	31.65	21.87
Bare ground	0.06	0.25	0.26	0.1	0.11	1.17
Rangeland	9.82	10.53	8.82	6.76	16.47	31.2
Surface area and population estimates						
Area (km^2)	488.7	218.2	645.6	213.0	105.01	205.86
Estimated population within the area (ppl)	71,111	49,291	148,557	17,404	48,161	100,582
Population density (ppl km^{-2})	145	225	230	81	458	488
LULC definitions per ESRI (Karra et al., 2021)						
Water – areas where water was present throughout the year. Excludes man-made structures like docks *Tree cover* – vegetation with closed/dense canopy ≥ 15 meters. *Flooded vegetation* – areas with intermixing of water and vegetation flooded seasonally or predominantly throughout the year.						

Crops – human planted vegetation (cereals, grasses, and corps) that are not at tree height.

Built area – human made structures like roads, rail road networks, parking spaces, industrial and residential buildings.

Bare ground – areas dominated by rocks, soil, sand (i.e. desert) with sparse to no vegetation throughout the year

Rangeland – homogeneous grasses, mixes of vegetation below tree-height with rocks and soil, clearings in the forests.

To assess the relationships between resistance and urbanization, we used LULC data at 10-meter resolution from ESRI (2017–2020) (Karra et al., 2021) and population density data at 100-meter resolution from World Population Hub (Bondarenko et al., 2020) (Table 1). We analyzed LULC and population density using QGIS 3.30.3 (QGIS Geographic Information System, 2024) equipped with a semi-automatic classification plug-in.

Further, because the resistance index was calculated for precipitation events across short time-scales (i.e., days), which underrepresents the draining time of some watersheds, we considered LULC and population density from a 10-km proximity zone surrounding monitoring locations (Table 1). For SFB NERR, we used 10-km proximity zones from San Pablo and Suisun embayments to quantify LULC and population density as is conventionally done at this watershed due to different hydrologic dynamics within each ebayment.

All data were collected using NERRS standard operating procedures. Briefly, water column DO (mg L^{-1}, calculated from % air saturation, temperature, and salinity at the time of measurement; thereby accounting for the impacts of temperature and salinity fluctuations on DO concentration), temperature, turbidity, salinity, and depth were measured at 15-min intervals using synchronized YSI-EXO2 multiparameter sondes. Meteorological conditions, including precipitation, were also measured at 15-min intervals using NERRS standard weather station instrumentation. PO_4^{3-}, NO_3^-, NH_4^+, NO_2^- and chlorophyll-*a* (Chl-*a*) were measured monthly from grab samples and analyzed in the lab (NERRS, 2023). Samples for nutrients were filtered in the field through 0.7 μm glass-fiber filters and analyzed following U.S. Environmental Protection Agency (EPA) methods (O'Dell, 1996b, a; U.S. EPA., 1993a). For Chl-*a* analysis, the samples were collected as whole water, then filtered onto 0.45 μm glass-filters and processed following APHA, (2001) and U.S. EPA., (1993b) methods. While Chl-*a* is also measured as Chlorophyll fluorescence using optical sensor with YSI sondes, NERRS recommends using laboratory-based measurements due to the confounding effects of various fluorescent species, organism type, light, temperature and more on sensor-based Chl-*a* measurements (sensor and lab-based measurements often do not correspond to each other). We omitted all data flagged as ‘suspect’ or ‘out of range’.

Additionally, we calculated water column depth as the sum of measured water depth plus the distance between the sonde and sediment bed (Table S1). We also calculated the sum of NO_3^-, NO_2^-, and NH_4^+ to assess dissolved inorganic nitrogen (DIN) concentrations and the ratio of DIN to PO_4^{-3} (hereafter, N:P).

2.2 Determination of major precipitation events.

Because hydrologic dynamics and related estuarine functions can vary dramatically with annual weather conditions, we first selected one ‘wet’ and one ‘dry’ year for each estuary using precipitation records from nearby airports. The purpose of selecting years with disparate rainfall patterns was to encompass the maximum range of variability in expected estuarine resistance to precipitation. Following Murrell et al. (2018), we calculated the long-term interquartile range (IQR, 1990-2020) of total monthly precipitation for each estuary and then selected relatively wet/dry years based on the number of months plotting above/below IQR and total annual precipitation. Possible wet and dry years were further filtered based on the completeness of NERRS data available for each estuary (Fig. S1). Long-term precipitation records included: Duluth International, Washington Reagan International, Jacksonville International, Birmingham Airport, and San Francisco International airports available from the National Center for Environmental Information.

Further, we selected major precipitation events within each wet and dry year by plotting daily precipitation using data from NERR meteorological stations (Fig. S2). Specifically, because the definition of ‘major’ precipitation events is hard to quantify and it varies across estuaries, we first considered hurricanes, tropical storms, Nor’easters, and other major storm events noted within NERR metadata sheets when selecting precipitation events. For example, at GTM we focused on tropical storms Colin, Julia, and Hermine, hurricanes Matthew and Irma, and two Nor'easters (Table S2). Data availability was a second consideration – we removed possible events for which there was a substantial amount of missing data. Lastly, because metabolic and hydrologic processes vary across seasons, we chose to focus on warm season events, with the exception of

San Francisco Bay where most precipitation occurs in the cool season but seasonal temperature fluctuations are generally lower than in other systems (Fig. S2 and S3, Table S2).

2.3 Calculation of resistance.

To investigate physicochemical and urban land-use characteristics associated with estuarine responses to precipitation events, we calculated the resistance index described in Orwin & Wardle (2004). The resistance index is a normalized parameter (−1 to +1) describing the magnitude of shift in a response variable from an initial condition. It has been used across a wide variety of ecosystems and response variables, including aquatic ecosystems (Thayne et al., 2022, 2023; Tsai et al., 2011). The resistance index is calculated as:

$$Resistance = 1 - \frac{2|D_0|}{(C_0 + |D_0|)} \quad \text{(eq. 1)}$$

where, C_0 = concentration of the response variable pre-disturbance, and D_0 = difference between the concentration of the response variable pre- and post-disturbance (P_0) (i.e., $D_0 = C_0 - P_0$). An index value of +1 indicates the highest possible resistance. Index values between 0 and 1 show that the magnitude of response variable shift is less than the magnitude of the baseline (i.e., $|D_0| \leq C_0$). A resistance index of 0 indicates that the shift in the response variable is equivalent to the magnitude of the baseline (i.e., $|D_0| = C_0$), whereas index values between < 0 and −1 reflect that change in the response variable is greater than the magnitude of the baseline (i.e., $|D_0| > C_0$). Overall, index values closer to 1 indicate more resistant systems (Orwin and Wardle, 2004).

While the resistance index is indicative of the ability of a system to maintain its pre-disturbance state, we emphasize that it is a normalized value that does not in itself convey information about overall estuarine health. Similarly, the resistance index in itself cannot infer if a shift has a positive or a negative effect on the ecosystem health. The resistance index can infer the ability of a system to maintain its pre-disturbance functions and/or ecological state (i.e., ecosystem stability). It enables the comparison of the amount of change induced by disturbance across vastly different estuaries. In parallel, it is also useful to consider the absolute value of the response variable (in this case DO) pre- and post-disturbance, which conveys information on the ambient state of an estuary and the directionality of its response to the disturbance. We therefore present C_0 and P_0 (Fig. 2a–e, Table S3) to define differences in DO within and across estuaries, as well as the resistance index, which pairs C_0 and P_0 values for the same event (Fig. 2f–j), to understand the ecosystem stability within and across estuaries after precipitation.

Because DO is critical to myriad functions that regulate the health of aquatic ecosystems (Abdul-Aziz et al., 2007; Abdul-Aziz & Gebreslase, 2023; Caffrey, 2004; Mulholland et al., 2001; Murrell et al., 2018; Odum, 1956) and because estuarine metabolism is virtually impossible to model due to bi-directional flow (Loken et al., 2021); we used temperature and salinity adjusted DO (mg L^{-1}) to calculate the resistance index. Additionally, the resistance index is highly sensitive to the researcher-defined baseline and post-disturbance time periods that are used to calculate C_0 and D_0. Therefore, we calculated C_0 as average DO during a manually-curated timespan preceding each precipitation event (~24 hours to 6 days, without precipitation) where DO dynamics looked unremarkable (Fig. S4, Table S2). The timespan for estimating P_0 was also manually selected in the context of each event, defined here as the maximum displacement from C_0 during and after the event (Fig. S4, Table S2). We also verified that the resistance index calculated using DO (mg L^{-1}) versus DO (% sat.) showed no notable differences (Fig. S5).

2.4 Statistical analysis.

To compare resistance, nutrient concentrations, and concentrations of DO pre- and post-precipitation within and between estuaries, we used ANOVA with post-hoc Tukey HSD or Kruskal-Wallis test, as appropriate based on the Shapiro-Wilk normality test.

To test associations of specific physicochemical and land-use factors with estuarine resistance to precipitation, we used linear regressions at continental and local scales independently (i.e., all estuaries combined vs. within each individual estuary) and within salinity-based groups (i.e., using a threshold of average annual salinity less than or above 10 ppt calculated for wet and dry years separately). The low salinity group included all LKS and CBM locations, First Mallard and Second Mallard locations at SFB during wet and dry years, as well as Fish River, Middle Bay, Magnolia Bay, and Weeks Bay (WB: during dry year only) at WKB estuary. The high salinity group included all monitoring locations at GTM, China Camp and Gallinas Creek at SFB estuary for wet and dry years, and Weeks Bay at WKB during the wet year. We used annual mean values for continental-scale, local-scale, and salinity-based groups regressions involving nutrients and Chl-*a* because monthly sampling intervals of lab-based measurements did not alway correspond with selected precipitation events. This resulted in two data points per monitoring location for nutrients and Chl-*a* regressions. While not directly associated with any particular precipitation event, relationships of nutrients and Chl-*a* with resistance values analyzed on an annual basis carry valuable information about how the ambient conditions of the system can impact an estuary's response to precipitation. This knowledge is essential for deriving and testing hypotheses that describe why a certain estuary may respond to a storm event in a particular way. For regressions involving sensor-based measurements, we attempted to provide as much resolution as possible into specific events. We therefore used values averaged over the event-specific baseline periods (Table S2) for sensor measurements across scales and salinity-based groupings. Values averaged over event-specific baseline periods were matched with corresponding event-specific resistance index resulting in one data point per precipitation event per each monitoring station. We did not include LULC and population density as predictors of resistance at individual estuaries because of the close proximity of some monitoring locations to one another (< 800 m).

Statistical analyses were performed in Python 3.10.11 using scipy.stats, statsmodels.stats.multicomp.pairwise_tukeyhsd, and seaborn.regplot packages.

3. Results

3.1 Land use/land cover and nutrient concentrations across estuaries.

Data describing LULC and population density within 10-km of the monitoring locations for all estuaries are shown in Table 1. Both embayments of the SFB had higher percentages of urban-type land characteristics (e.g., built area) and population density than any other estuary, followed by CBM (Table 1). Agricultural land was more prevalent at WKB (30.36%) compared to other estuaries. GTM and LKS had more mixed LULC, with high proportions of tree cover. With regard to nutrient concentrations, SFB and CBM had high DIN concentrations compared to LKS and GTM ($p < 0.01$). Mean DIN values at all SFB and CBM monitoring locations were > 0.504 mg-N L^{-1} versus < 0.16 mg-N L^{-1} at LKS and GTM (Fig. S6). Phosphate concentrations were the highest at SFB (mean across all monitoring locations = 0.135 mg-P L^{-1}, SD = 0.08; means at all other estuaries < 0.03 mg-P L^{-1}, $p < 0.001$, Fig. S5). Overall, mean N:P across LKS, CBM, GTM, WKB, and SFB estuaries were 28.04 (SD = 28.08), 26.56 (SD = 10.75), 2.84 (SD = 0.91), 83.82 (SD = 55.27), and 5.10 (SD = 1.4), respectively (Fig. S7), with GTM and SFB indicating N limiting conditions based on a 16N:1P Redfield ratio (Redfield, 1934).

3.2 Changes in dissolved oxygen and resistance to precipitation across estuaries and monitoring locations.

DO concentrations pre- and post-precipitation differed across all estuaries, when evaluating the overall trends (pre- (C_0): F = 45.6, $p < 0.0001$; and post- (P_0): F = 17.1, $p < 0.0001$, Fig. 2a–e). Across all precipitation events (i.e., non-specific to an event), SFB had the highest pre-precipitation DO concentration of all estuaries. Generally, at SFB and CBM (more urban) and at WKB (more agricultural), DO declined following precipitation ($p < 0.01$). At LKS, precipitation events significantly increased DO concentration (F = 5.1, $p = 0.027$). There was no significant difference between the overall pre- and post-precipitation DO concentrations at GTM (F = 0.5, $p = 0.48$).

Resistance also differed across estuaries (F = 21.6, df1 = 4, df2 = 172, $p < 0.0001$, Fig. 2). SFB monitoring locations had the highest mean resistance to precipitation (mean = 0.68), while monitoring locations at LKS were the least resistant to precipitation (mean = 0.47). Within individual estuaries, resistance varied across monitoring locations at LKS (F = 13.9, df1 = 3, df2 = 24, $p < 0.0001$), CBM (F = 7.9, df1 = 2, df2 = 27, $p < 0.01$), and SFB (F = 10.2, df1 = 3, df2 = 27, $p < 0.001$) but was not significantly different between monitoring locations within GTM (F = 3.5, df = 3, $p = 0.32$), WKB (F = 0.9, df = 3, $p = 0.81$) (Fig. 2f–j). Resistance was most variable across monitoring locations at LKS (−0.26 to 0.89) and least variable across locations at WKB (0 to 0.73).

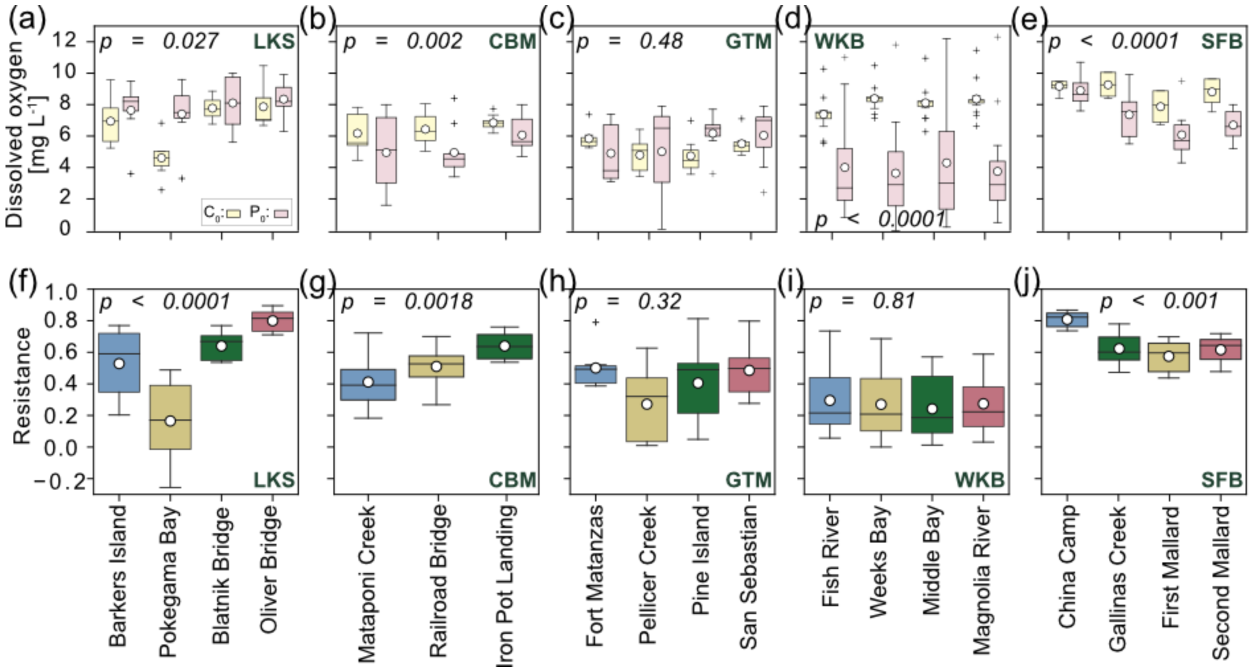

Figure 2: Variation in pre- and post-disturbance distribution of dissolved oxygen and resistance within individual estuaries. Boxes show the quartiles of the dataset and the whiskers show the rest of the distribution. Means are shown in white circles, and medians are shown in black solid lines. *P*-values are at the top of each panel. a-e) Distribution of dissolved oxygen concentrations prior to (C_0, solid boxes) and post (P_0, dashed boxes) precipitation. f-j) Resistance index across monitoring locations at: Lake Superior (LKS) NERR (all n = 7), Chesapeake Bay (CBM) NERR (all n = 10), Guana Tolomato-Matanzas (GTM) NERR (all n = 7), Weeks Bay (WKB) NERR (all n = 15), San Francisco Bay (SFB) NERR (n = 8 except Second Mallard (SM) n = 7).

3.3 Continental, salinity-based, and local relationships of resistance with physicochemical factors, land use/land cover, and population density.

When data from the five estuaries were considered together (i.e., continental-scale), we found significant positive relationships of resistance with water column depth ($p < 0.0001$; $R^2 = 0.10$), turbidity ($p = 0.0015$; $R^2 = 0.06$), log(DIN) ($p = 0.031$; $R^2 = 0.12$), percent built area ($p = 0.02$; $R^2 = 0.14$), and population density ($p = 0.001$; $R^2 = 0.27$); and significant negative relationships to water temperature ($p < 0.0001$; $R^2 = 0.39$) and Chl-*a* ($p < 0.0001$; $R^2 = 0.39$) (Fig. 3, Table S4).

When grouped by salinity, estuarine resistance to precipitation was more tightly correlated to physicochemical and land-use factors (Fig. 3, Table S4). Within 'low-salinity' estuaries, resistance was positively related with depth of the water column ($p < 0.0001$; $R^2 = 0.1$), which is consistent with the trend observed on continental-scale; and negatively related to salinity ($p < 0.0001$; $R^2 = 0.214$), a relationship not found on continental-scale. Within 'high-salinity' estuaries, mean resistance showed positive relationships to annual mean log(DIN) ($p = 0.004$; $R^2 = 0.55$) and to percent built area ($p = 0.0002$, $R^2 = 0.73$), which also was consistent with continental-scale results. Also, resistance in high-salinity estuaries was positively associated with turbidity ($p < 0.0001$, $R^2 = 0.29$). Observations present in 'high-salinity' estuaries but absent from continental-scale evaluations included negative relationships of mean resistance with tree cover ($p = 0.011$; $R^2 = 0.46$), and negative relationships to N:P ($p < 0.0001$; $R^2 = 0.81$). Additionally, mean resistance in both low- and high-salinity groups was positively related to population density ($p = 0.051$; $R^2 = 0.16$, and $p = 0.0002$; $R^2 = 0.73$, respectively), and negatively related to water temperature ($p = 0.001$; $R^2 = 0.38$, and $p = 0.002$; $R^2 = 0.6$, respectively) and Chl-*a* ($p = 0.0002$, $R^2 = 0.46$, and $p = 0.044$; $R^2 = 0.32$, respectively). The temperature and Chl-*a* trends were consistent with continental-scale observations. Generally, 'low-salinity' estuaries showed fewer relationships of resistance with physicochemical factors, LULC, and population density compared to 'high-salinity' estuaries.

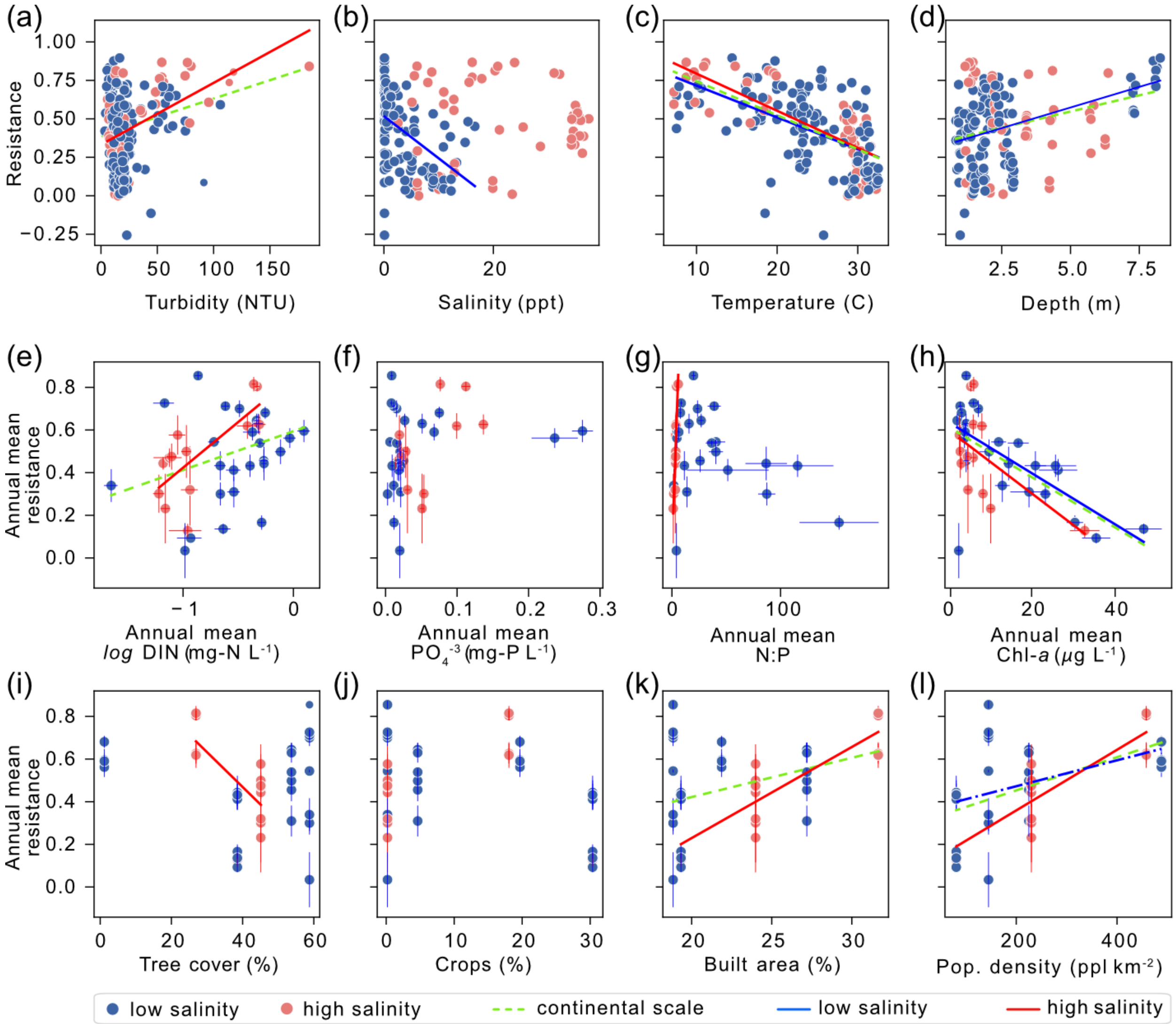

Figure 3. Relationships of continental-scale and salinity-based resistance with physicochemical factors, land use/land cover, and population density. Continental-scale regressions considered all monitoring locations across all estuaries. Significant relationships ($p < 0.05$) are shown in green, red, and blue for continental-scale, high-salinity and low-salinity estuaries, respectively. Standard errors of the mean are shown in vertical and horizontal lines. The LULC parameters and population density were used from within the 10-km radius adjoined to the monitoring locations. Please refer to Table S4 for resulting statistics and to Fig. S8 for information on covariance among predictor variables.

At local scales (i.e., within each estuary), resistance was related to some physicochemical factors that were not observed in continental-scale or salinity-based relationships. Moreover, the number, strength, and trends of relationships between local-scale resistance and physicochemical factors varied substantially across estuaries (Fig. 4, Figs. S9, S10). Resistance at GTM had the most relationships to physicochemical factors. It was negatively related to water temperature ($p < 0.001$; $R^2 = 0.52$), PO_4^{-3} ($p = 0.013$; $R^2 = 0.67$) and Chl-*a* concentrations ($p = 0.009$; $R^2 = 0.71$); and positively related to salinity and N:P ($p = 0.02$, $R^2 = 0.19$ and $p = 0.009$, $R^2 = 0.71$, respectively). In contrast, at CBM, resistance was related only to water column depth (positive, $p = 0.013$; $R^2 = 0.21$). At LKS, resistance was positively related to water column depth ($p < 0.0001$; $R^2 = 0.5$), and negatively related to turbidity ($p = 0.004$; $R^2 = 0.28$). At WKB, relationships of resistance with water temperature, salinity, and Chl-*a* concentrations were all negative ($p < 0.0001$, $R^2 = 0.30$; $p = 0.013$, $R^2 = 0.1$; and $p = 0.015$, $R^2 = 0.66$, respectively). At SFB, resistance was negatively related to water column depth ($p < 0.0001$; $R^2 = 0.48$), which opposed the general trend, and positively related to salinity ($p = 0.00016$; $R^2 = 0.42$). There was no overarching relationship between resistance and total precipitation amount of each event, except for a significant but weak negative relationship at GTM estuary ($p = 0.026$, $R^2 = 0.18$, Fig. S11).

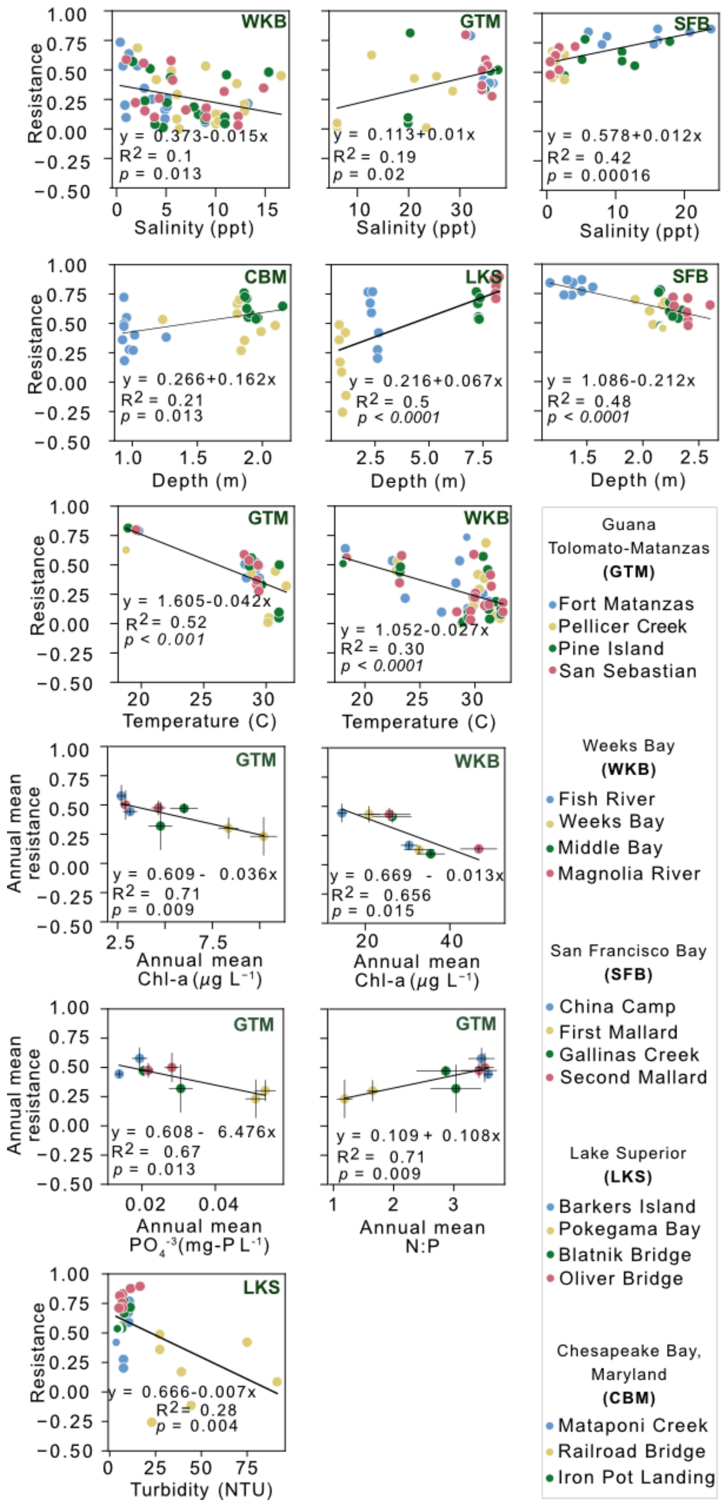

Figure 4. Relationships between resistance and physicochemical factors for each estuary. National Estuarine Reserve System (NERR) estuary abbreviations: Lake Superior (LKS) NERR, Chesapeake Bay, Maryland (CBM) NERR, Guana Tolomato Matanzas (GTM) NERR, Weeks Bay (WKB) NERR, and San Francisco Bay (SFB) NERR. Significant correlations ($p < 0.05$) are shown

with black lines. Standard errors of the mean are shown in vertical and horizontal black lines for relationships using annual means for chlorophyll-*a* (Chl-*a*), PO_4^{3-}, and N:P. For additional results see Figs. S9, S10, and S12.

In summary, some relationships of estuarine resistance with physicochemical factors and urban land use appeared to be more universal while others varied across scales (Fig. 5). For instance, resistance was related to water temperature, water column depth, turbidity, and Chl-*a* across continental- and local-scales, and within salinity-based estuary groups. Dissolved inorganic N, percent built area, and population density were all related to resistance at the continental scale and in salinity-based groups. Both local and salinity-based evaluations revealed correlations of N:P, salinity, and turbidity with resistance to precipitation. Unique relationships included PO_4^{-3} at the local scale (GTM only) and tree cover in 'high-salinity' estuaries.

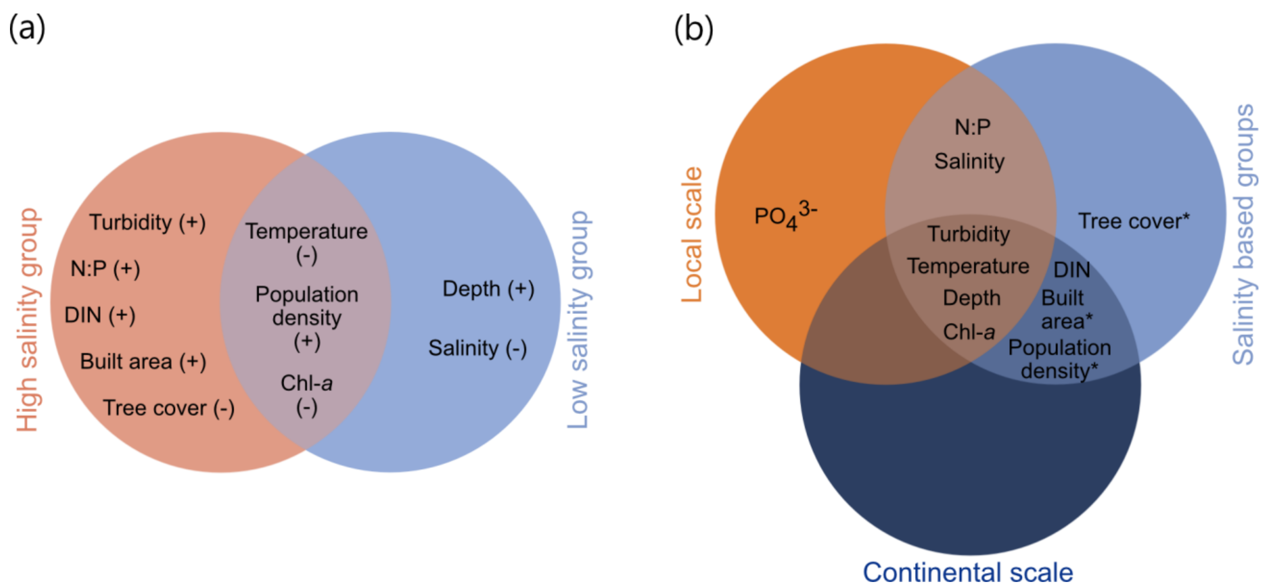

Figure 5. Cross-scale relationships of estuarine resistance with physicochemical factors and land-use characteristics. a) Venn diagram of resistance relationships to physicochemical factors and land-use characteristics in high- vs. low-salinity estuaries. Positive or negative relationships are indicated with '+' and '–' respectively. b) Venn diagram of resistance relationships with physicochemical and land-use factors in continental, local, and salinity-based groups. Estuarine resistance with land use/land cover and population density marked with asterisks (*) were not evaluated at local-scale due to overlap in the spatial domains of some monitoring locations.

4. Discussion

Understanding patterns in estuarine responses to precipitation is important for predicting the impacts of urbanization and climate change on estuaries as a whole. Previous studies have shown that patterns identified at large scales may not be applicable across different climatic conditions, regional geology, and other ecosystem factors (Baker et al., 2004; Gannon et al., 2022; Hopkins et al., 2015; Kaushal et al., 2018; Ombadi and Varadharajan, 2022; Poff et al., 2006). Our results underscore the importance of cross-scale evaluations that can elucidate commonalities in estuarine response to precipitation, as well as variability in the factors associated with resistance to precipitation across individual estuaries.

We show that while relationships between estuarine resistance, urbanization, and DIN may prevail at the continental-scale, they may not correspond to resistance in individual estuaries. This is because local resistance is associated with myriad specific factors in addition to many factors identified at larger scales. Also, in contrast to our overarching hypothesis, we find that urbanized estuaries tend to have higher resistance than more pristine estuaries. These results could suggest that the effects of watershed urbanization may impact estuarine stability by either providing some mechanism that allows estuaries responding to major precipitation events to dampen large shifts in DO; or by disturbing the baseline DO to an extent where even a major precipitation event would not produce a significant shift in DO, making the system appear highly resistant.

4.1 Dissolved oxygen dynamics differ in estuaries with urban or agricultural land use/land cover

There were vast differences in geometry, circulation, and hydrologic conditions among urbanized estuaries versus estuaries surrounded by agricultural land in this study. Yet, they exhibited similar patterns in DO response to precipitation. Precipitation generally reduced DO concentrations at WKB, SFB, and CBM (Fig. 2a–e). Simultaneously, the estuary with the least amount of urbanized LULC – LKS – overall, experienced an increase in DO concentration following precipitation.

While a wide range of physical factors can impact DO in estuaries including channel geometry and river discharge (Kemp and Boynton, 1980; Raymond et al., 2012; Raymond and Cole, 2001), wind (Scully, 2010; Zheng et al., 2024), and circulation (Raimonet & Cloern, 2017), urban estuaries in particular are often impacted by a combination of these processes. Urban estuaries often serve as basins for wastewater treatment outflows, which can supply continued freshwater discharge and nutrients when river discharge is low. Both urban and agriculturally influenced estuaries are prone to increased nutrient loading during and shortly after precipitation events (Chapin et al., 2004; Costanzo et al., 2003; Mallin et al., 2009), which impacts primary production and microbial metabolism and may lead to declines in DO concentrations (e.g., algal blooms).

Therefore, closely examining the directionality of change in DO response to precipitation is important for informing the environmental significance of storm events for a specific system. An overall increase in DO following precipitation could reduce hypoxia through processes like reaeration of the water column (Bianucci et al., 2018; Bohórquez-Bedoya et al., 2024) and have positive effects on nutrient cycling (Harris et al., 2015) and growth conditions for macro- and micro- fauna. A decrease in DO following precipitation may reflect the opposite effects (e.g., hypoxia), which are associated with changes in microbial community structure, disruptions in nutrient cycles, and fish die-off (Diaz et al., 1992; Llansó, 1992). Further, the degree to which ecosystem health is associated with DO changes is intertwined with its original ecological state and with the magnitude of change in DO. An increase in DO following a storm may be less consequential for estuaries with DO-replete ambient conditions as compared to estuaries with chronically depleted DO. This implies that to more fully assess the effects of storms on estuarine ecosystem stability and health, estuarine responses should be evaluated both through the lens of the resistance index, historical DO conditions and through the magnitude and directionality of DO change.

For example, resistance index values for the more pristine and tree-cover dominated Pokegama Bay at LKS was comparable to most monitoring stations at WKB, which were associated with agriculture; however, Pokegama Bay and WKB experienced different patterns in DO change following precipitation (Figs. 2, S4). While the full nature of the causes and impacts of DO change in each estuary is beyond the scope of this study, the differences in absolute DO change suggests that different underlying processes influence stability in estuarine dynamics in response to precipitation across different estuaries. Our goal here is to unravel common factors that are able to predict estuarine resistance at the continental-scale, despite this variation in processes, as well as to reveal specific predictors in estuaries with contrasting salinity and in individual estuaries to help elucidate certain dynamics that may be more impactful in one estuary relative to another.

4.2 Urbanization and inorganic nitrogen correspond with elevated resistance to precipitation at the continental-scale.

Higher resistance to precipitation in the most urbanized estuaries and overarching relationships of urban LULC with resistance across all estuaries reflect that estuaries within urban watersheds typically experience relatively small shifts in DO following precipitation (Figs. 2-3). These results contradict our hypothesis that urban estuaries should show low resistance to precipitation because of greater physical and chemical disturbances (flashiness, streambed scouring, N loading, turbidity, etc.) (Bernhardt et al., 2008; Groffman et al., 2004; Hession et al., 2003; Hopkinson & Vallino, 1995; Walsh et al., 2005).

It is possible that watershed urbanization could equip estuaries with adaptations that help dampen precipitation impacts on shifts in DO. For instance, an increase in flashiness in waterways would increase flow velocity and reaeration of the water column in estuaries (Raymond et al., 2012; Raymond and Cole, 2001) and contribute to phytoplankton removal via transport or turbidity-driven light attenuation (Caffrey, 2004; Pennock and Sharp, 1986). This impact may be particularly important for estuaries whose baseline conditions are influenced by algal blooms, which induce large DO fluctuations by overproducing DO during the day and severely depleting DO at night (Chapin et al., 2004; Ni et al., 2020). Such control for overgrowth of phytoplankton would help maintain DO near baseline. Supporting this explanation, turbidity-driven limitations on phytoplankton were previously reported for the SFB estuary (Cloern, 1987). We also found positive and negative relationships of turbidity and Chl-*a*, respectively, with built area and population density (Fig. S13).

Relatively high levels of ambient N and low ambient DO in urban estuaries may also facilitate comparatively low DO fluctuations in response to precipitation. Watershed urbanization is often related to high N export to estuarine environments including in the San Francisco Bay area (Bettez et al., 2015; Dugdale et al., 2007; Hopkinson and Vallino, 1995; Parker et al., 2012; Reisinger et al., 2016). Here, estuarine inorganic N concentrations were related to urbanization and also were a major predictor of resistance at the continental-scale (Figs. 3 and S13). While moderate levels of N support biological metabolisms (Howarth, 1988; Howarth and Marino, 2006;

Vitousek and Howarth, 1991; Zhang et al., 2021), nutrient loading is a significant problem for urban aquatic environments (Beman et al., 2005; Bernot et al., 2010; Black et al., 2011; Mulholland et al., 2008). For urban estuaries, where N loading is associated with chronically low DO availability, this could mean that precipitation-driven increases in DO under simultaneous high N input would be small, which would result in higher resistance. Nitrogen limitation, in contrast, is prevalent in coastal marine systems and can negatively impact overall estuarine health by constraining biological activity (Elser et al., 2007; Guildford and Hecky, 2000; Paerl, 2018; Paerl and Piehler, 2008). Relationships of resistance with N and urbanization were particularly evident in more coastal (high-salinity) estuaries where we found positive associations of resistance with N:P and built area (Fig. 3). Thus, altered N dynamics in urban estuaries may be key to understanding their comparatively low change in response to precipitation.

Alternatively, we also consider if baseline DO concentrations in urban estuaries are already disturbed to such an extent that precipitation events cause minimal further disruption. Urbanization itself can promote large diel DO fluctuations, as suggested by (Gold et al., 2020), and if a precipitation event induces fluctuations that are similar in magnitude, post-precipitation DO concentrations will not deviate significantly from baseline conditions. Under such a scenario, urban estuaries will appear more resistant to precipitation events compared to more natural estuaries.

4.3 Water column depth, temperature, turbidity, and Chl-*a* are related to resistance across all scales.

We found generalizable patterns (across all scales), in which resistance was mostly positively related to water column depth and turbidity, and negatively related to water temperature and Chl-*a* (Figs. 3–5). As discussed above, phytoplankton dynamics may be an important factor in regulating DO in response to disturbance due to their tight linkage with N loading, which is consistent with results previously reported by others (Thayne et al., 2023). This is further underscored by the existence of a relationship between Chl-*a* and resistance across continental, salinity-based, and local analyses. In parallel, the relationship between resistance and turbidity was positive at the continental scale and in the high salinity group (Fig. 3), while at LKS resistance and turbidity correlated negatively (Figs. 3, 4). The positive associations of resistance with turbidity and simultaneous negative relationship with Chl-*a* can be attributed to turbidity-driven light attenuating conditions that restrict phytoplankton growth, which is further confirmed through negative correlation between turbidity and Chl-*a* (Fig. S8).

Water column depth can also influence the calculated resistance of estuaries to precipitation through physical and hydrologic impacts on DO. Through dilution, deeper estuaries could have a greater capacity to resist hydrologic changes in response to precipitation, for instance by attenuating the influx of oxygen-saturated rain water; nutrient loading; turbulence; and water-atmosphere gas exchange. Similarly, deep estuaries have longer equilibration time with environmental conditions and less diel variability in parameters like temperature (Caissie, 2006; Macan, 1958), which also affects diel and seasonal DO dynamics, possibly resulting in more stable DO baselines and more moderate responses to precipitation. Deeper estuaries can also be associated with urbanization, which also shows high resistance in this study, because shifts towards more urban and agricultural LULC generally deepen estuarine channels through increased runoff, sediment transport, hydrological flashiness, channel dredging, and/or other anthropogenic activities (O'Driscoll et al., 2010; Simon and Rinaldi, 2006; Walsh et al., 2005). Therefore, water column depth appears to be a critical factor in regulating the resistance to precipitation in estuaries.

Lastly, because temperature controls various chemical and biological processes that impact DO availability (e.g., microbial growth, oxygen solubility), many studies have focused on the impact of rising temperature on DO dynamics in estuaries (Apple et al., 2006; Caffrey, 2003; Caffrey et al., 2014). Highlighted results link climate change to thermal pollution of aquatic systems following rain events (Zahn et al., 2021) and show connections of elevated global temperatures with decreased primary production (Song et al., 2018). As such, estuaries with elevated ambient temperatures may have a decreased capacity to resist disturbances to DO dynamics relative to estuaries with more moderate temperatures.

4.4 High variability in factors associated with resistance at local scales.

The contrasting relationships between physicochemical factors and resistance across monitoring locations in individual estuaries highlight substantial fine-scale variation in precipitation responses (Fig. 4). For example, resistance at CBM is related to one factor (water column depth), while at GTM, resistance is related to five factors. The variability in factors associated with resistance suggests that individual estuaries may need to consider factors beyond water temperature, water column depth, turbidity, and Chl-*a* in water-quality management and conservation strategies. For instance, Chl-*a* and dissolved inorganic phosphorus have been shown to respond to storms in some estuaries more than in others due to differences in light limitation, grazing, and nutrient concentrations (Chen et al., 2015; Cloern, 2001; Cloern and Jassby, 2010; Dix et al., 2013, 2008; Liao et al., 2021; Zhang et al., 2022). Likewise, water temperature and salinity also have variable responses to precipitation (Buelo et al., 2023; Chen et al., 2015; Dix et al., 2008), leading to differences in biological processes and phytoplankton activity in different estuaries (Apple et al., 2008). While there are myriad potential estuary-specific interactions that may result in different responses to stressors, our results highlight that system-variability is important when identifying parameters involved in estuarine resistance to precipitation. We also acknowledge that other scales of investigation (e.g., regional) could introduce additional insight into the predictors of estuarine resistance. Moreover, system dependencies on groundwater discharge as a driver of nutrient dynamics and control on DO dynamics (Brookfield et al., 2021; Kornelsen and Coulibaly, 2014) as well as system dependencies on microbial community structure (Cheng et al., 2021) should also be appraised when evaluating resistance of urban estuaries to precipitation.

5. Conclusions

In light of increasing urbanization and emerging climatic scenarios, cross-scale evaluations of the responses of estuaries to precipitation events are imperative for developing effective management strategies. We find that urban estuaries appear to be more resistant to changes in DO in response to precipitation than more pristine estuaries; and that the depth of the water column, water temperature, turbidity, and Chl-*a* are generalizable cross-scale predictors for estuarine resistance. However across different scales, we find that system variability results in additional factors that are important to consider when managing the responses to major precipitations events of individual estuaries. Based on our results, we suggest that investigations targeting N, nutrient delivery mechanisms, and microbial activity could help understand what makes urban estuaries more resistant to large shifts in DO following precipitation. We also highlight that high-resolution water quality and nutrient data surrounding precipitation events, along with careful considerations of local variabilities and models for system responses to precipitation, are needed to help elucidate the underlying mechanisms for high resistance of urban estuaries. This study serves as a platform for improvement of guidelines and predictive capabilities addressing system response to future climatic and urbanization scenarios.

Data availability: This study used publicly available datasets, which included: 1) Long-term estuarine water quality, nutrients and meteorological conditions and watershed boundaries for Lake Superior (LKS) NERR, Chesapeake Bay, Maryland (CBM) NERR, Guana Tolomato Matanzas (GTM) NERR, Weeks Bay (WKB) NERR, and San Francisco Bay (SFB) NERR stations from https://cdmo.baruch.sc.edu; 2) Long-term precipitation data from U.S. airports from https://www.ncei.noaa.gov/cdo-web/datasets; 3) Land use/land cover maps from https://livingatlas.arcgis.com/landcover/; 4) U.S. population data from https://www.worldpop.org/. Data and data processing code are also available at https://figshare.com/s/49d2f3dca084d885638a.

Author Contribution: E.B.G. and A.B.T. developed the study and interpreted the results. A.B.T. performed data analysis and drafted the manuscript. All authors contributed to manuscript editing.

Competing interest: The authors declare that they have no competing interest.

Acknowledgements

This material is based upon work supported by the U.S. Department of Energy, Office of Science, Biological and Environmental Research program Early Career award to EBG. The work was performed by Pacific Northwest National Laboratory, operated by Battelle Memorial Institute for the U.S. Department of Energy under Contract DE-AC05-76RL01830. We thank the National Estuarine Research Reserve System (NERRS), supported by awards from the Office for Coastal Management, National Oceanographic and Atmospheric Administration (NOAA), and Kyle Derby and Dr. Scott Phipps from Chesapeake Bay, Maryland NERR and Weeks Bay NERR, respectively, for maintaining water quality monitoring stations and providing publicly available data upon which this publication is based. We also thank Drs. Alexander J. Reisinger and Matthew H. Kaufman for the insight on metabolism models for aquatic environments.

References

Abdul-Aziz, O. I. and Gebreslase, A. K.: Emergent Scaling of Dissolved Oxygen (DO) in Freshwater Streams Across Contiguous USA, Water Resour. Res., 59, e2022WR032114, https://doi.org/10.1029/2022WR032114, 2023.
Abdul-Aziz, O. I., Wilson, B. N., and Gulliver, J. S.: Calibration and Validation of an Empirical Dissolved Oxygen Model, J. Environ. Eng., 133, 698–710, https://doi.org/10.1061/(ASCE)0733-9372(2007)133:7(698), 2007.
APHA: Standard Methods for the Examination of Water and Wastewater, (SM10200H), 20th ed., United Book Press, Inc., Baltimore, Maryland, 2001.
Apple, J. K., Giorgio, P. A. del, and Kemp, W. M.: Temperature regulation of bacterial production, respiration, and growth efficiency in a temperate salt-marsh estuary, Aquat. Microb. Ecol., 43, 243–254, https://doi.org/10.3354/ame043243, 2006.
Apple, J. K., Smith, E. M., and Boyd, T. J.: Temperature, Salinity, Nutrients, and the Covariation of Bacterial Production and Chlorophyll-a in Estuarine Ecosystems, J. Coast. Res., 2008, 59–75, https://doi.org/10.2112/SI55-005.1, 2008.
Baker, D. B., Richards, R. P., Loftus, T. T., and Kramer, J. W.: A New Flashiness Index: Characteristics and Applications to Midwestern Rivers and Streams1, JAWRA J. Am. Water Resour. Assoc., 40, 503–522, https://doi.org/10.1111/j.1752-1688.2004.tb01046.x, 2004.
Beman, M. J., Arrigo, K. R., and Matson, P. A.: Agricultural runoff fuels large phytoplankton blooms in vulnerable areas of the ocean, Nature, 434, 211–214, https://doi.org/10.1038/nature03370, 2005.
Bernhardt, E. S., Band, L. E., Walsh, C. J., and Berke, P. E.: Understanding, Managing, and Minimizing Urban Impacts on Surface Water Nitrogen Loading, Ann. N. Y. Acad. Sci., 1134, 61–96, https://doi.org/10.1196/annals.1439.014, 2008.
Bernhardt, E. S., Heffernan, J. B., Grimm, N. B., Stanley, E. H., Harvey, J. W., Arroita, M., Appling, A. P., Cohen, M. J., McDowell, W. H., Hall Jr., R. O., Read, J. S., Roberts, B. J., Stets, E. G., and Yackulic, C. B.: The metabolic regimes of flowing waters, Limnol. Oceanogr., 63, S99–S118, https://doi.org/10.1002/lno.10726, 2018.
Bernot, M. J., Sobota, D. J., Hall Jr, R. O., Mulholland, P. J., Dodds, W. K., Webster, J. R., Tank, J. L., Ashkenas, L. R., Cooper, L. W., Dahm, C. N., Gregory, S. V., Grimm, N. B., Hamilton, S. K., Johnson, S. L., Mcdowell, W. H., Meyer, J. L., Peterson, B., Poole, G. C., Valett, H. M., Arango, C., Beaulieu, J. J., Burgin, A. J., Crenshaw, C., Helton, A. M., Johnson, L., Merriam, J., Niederlehner, B. R., O'brien, J. M., Potter, J. D., Sheibley, R. W., Thomas, S. M., and Wilson, K.: Inter-regional comparison of land-use effects on stream metabolism, Freshw. Biol., 55, 1874–1890, https://doi.org/10.1111/j.1365-2427.2010.02422.x, 2010.
Bettez, N. D., Duncan, J. M., Groffman, P. M., Band, L. E., O'neil-dunne, J., Kaushal, S. S., Belt, K. T., and Law, N.: Climate Variation Overwhelms Efforts to Reduce Nitrogen Delivery to Coastal Waters, Ecosystems, 18, 1319–1331, https://doi.org/10.1007/s10021-015-9902-9, 2015.
Bianchi, T. S.: Biogeochemistry of Estuaries, Oxford University Press, USA, 721 pp., 2007.
Bianucci, L., Balaguru, K., Smith, R. W., Leung, L. R., and Moriarty, J. M.: Contribution of hurricane-induced sediment resuspension to coastal oxygen dynamics, Sci. Rep., 8, 15740, https://doi.org/10.1038/s41598-018-33640-3, 2018.
Black, R. W., Moran, P. W., and Frankforter, J. D.: Response of algal metrics to nutrients and physical factors and identification of nutrient thresholds in agricultural streams, Environ. Monit. Assess., 175, 397–417, https://doi.org/10.1007/s10661-010-1539-8, 2011.
Bohórquez-Bedoya, E., Rovelli, L., and Lorke, A.: Rainfall as a driver for near-surface turbulence and air-water gas exchange in freshwater aquatic systems, PLOS ONE, 19, e0299998, https://doi.org/10.1371/journal.pone.0299998, 2024.
Bondarenko, M., Kerr, D., Sorichetta, A., and Tatem, A.: Census/projection-disaggregated gridded population datasets for 189 countries in 2020 using Built-Settlement Growth Model (BSGM) outputs, https://doi.org/10.5258/SOTON/WP00684, 2020.
Booth, D. B. and Jackson, C. R.: Urbanization of Aquatic Systems: Degradation Thresholds, Stormwater Detection, and the Limits of Mitigation1, JAWRA J. Am. Water Resour. Assoc., 33, 1077–1090,

https://doi.org/10.1111/j.1752-1688.1997.tb04126.x, 1997.

Brookfield, A. E., Hansen, A. T., Sullivan, P. L., Czuba, J. A., Kirk, M. F., Li, L., Newcomer, M. E., and Wilkinson, G.: Predicting algal blooms: Are we overlooking groundwater?, Sci. Total Environ., 769, 144442, https://doi.org/10.1016/j.scitotenv.2020.144442, 2021.

Buelo, C. D., Besterman, A. F., Walter, J. A., Pace, M. L., Ha, D. T., and Tassone, S. J.: Quantifying Disturbance and Recovery in Estuaries: Tropical Cyclones and High-Frequency Measures of Oxygen and Salinity, Estuaries Coasts, https://doi.org/10.1007/s12237-023-01255-1, 2023.

Caffrey, J. M.: Production, Respiration and Net Ecosystem Metabolism in U.S. Estuaries, in: Coastal Monitoring through Partnerships: Proceedings of the Fifth Symposium on the Environmental Monitoring and Assessment Program (EMAP) Pensacola Beach, FL, U.S.A., April 24–27, 2001, edited by: Melzian, B. D., Engle, V., McAlister, M., Sandhu, S., and Eads, L. K., Springer Netherlands, Dordrecht, 207–219, https://doi.org/10.1007/978-94-017-0299-7_19, 2003.

Caffrey, J. M.: Factors controlling net ecosystem metabolism in U.S. estuaries, Estuaries, 27, 90–101, https://doi.org/10.1007/BF02803563, 2004.

Caffrey, J. M., Murrell, M. C., Amacker, K. S., Harper, J. W., Phipps, S., and Woodrey, M. S.: Seasonal and Inter-annual Patterns in Primary Production, Respiration, and Net Ecosystem Metabolism in Three Estuaries in the Northeast Gulf of Mexico, Estuaries Coasts, 37, 222–241, https://doi.org/10.1007/s12237-013-9701-5, 2014.

Caissie, D.: The thermal regime of rivers: a review, Freshw. Biol., 51, 1389–1406, https://doi.org/10.1111/j.1365-2427.2006.01597.x, 2006.

Chang, H.: Spatial and Temporal Variations of Water Quality in the Han River and Its Tributaries, Seoul, Korea, 1993–2002, Water. Air. Soil Pollut., 161, 267–284, https://doi.org/10.1007/s11270-005-4286-7, 2005.

Chapin, T. P., Caffrey, J. M., Jannasch, H. W., Coletti, L. J., Haskins, J. C., and Johnson, K. S.: Nitrate sources and sinks in Elkhorn Slough, California: Results from long-term continuous in situ nitrate analyzers, Estuaries, 27, 882–894, https://doi.org/10.1007/BF02912049, 2004.

Chapra, S. C.: Surface Water-Quality Modeling, Waveland Press, 865 pp., 2008.

Chen, N., Wu, Y., Chen, Z., and Hong, H.: Phosphorus export during storm events from a human perturbed watershed, southeast China: Implications for coastal ecology, Estuar. Coast. Shelf Sci., 166, 178–188, https://doi.org/10.1016/j.ecss.2015.03.023, 2015.

Cheng, Y., Bhoot, V. N., Kumbier, K., Sison-Mangus, M. P., Brown, J. B., Kudela, R., and Newcomer, M. E.: A novel random forest approach to revealing interactions and controls on chlorophyll concentration and bacterial communities during coastal phytoplankton blooms, Sci. Rep., 11, 19944, https://doi.org/10.1038/s41598-021-98110-9, 2021.

Cloern, J. E.: Turbidity as a control on phytoplankton biomass and productivity in estuaries, Cont. Shelf Res., 7, 1367–1381, https://doi.org/10.1016/0278-4343(87)90042-2, 1987.

Cloern, J. E.: Our evolving conceptual model of the coastal eutrophication problem, Mar. Ecol. Prog. Ser., 210, 223–253, https://doi.org/10.3354/meps210223, 2001.

Cloern, J. E. and Jassby, A. D.: Patterns and Scales of Phytoplankton Variability in Estuarine–Coastal Ecosystems, Estuaries Coasts, 33, 230–241, https://doi.org/10.1007/s12237-009-9195-3, 2010.

Costanzo, S. D., O'Donohue, M. J., and Dennison, W. C.: Assessing the seasonal influence of sewage and agricultural nutrient inputs in a subtropical river estuary, Estuaries, 26, 857–865, https://doi.org/10.1007/BF02803344, 2003.

Cox, B.: A review of currently available in-stream water-quality models and their applicability for simulating dissolved oxygen in lowland rivers, Sci. Total Environ., 314–316, 335–377, https://doi.org/10.1016/S0048-9697(03)00063-9, 2003.

Diaz, R. J., Neubauer, R. J., Schaffner, L. C., Pihl, L., and Baden, S. P.: Continuous monitoring of dissolved oxygen in an estuary experiencing periodic hypoxia and the effect of hypoxia on macrobenthos and fish, in: Marine Coastal Eutrophication, edited by: Vollenweider, R. A., Marchetti, R., and Viviani, R., Elsevier, Amsterdam, 1055–1068, https://doi.org/10.1016/B978-0-444-89990-3.50091-2, 1992.

Dix, N., Phlips, E., and Suscy, P.: Factors Controlling Phytoplankton Biomass in a Subtropical Coastal

Lagoon: Relative Scales of Influence, Estuaries Coasts, 36, 981–996, https://doi.org/10.1007/s12237-013-9613-4, 2013.

Dix, N. G., Phlips, E. J., and Gleeson, R. A.: Water Quality Changes in the Guana Tolomato Matanzas National Estuarine Research Reserve, Florida, Associated with Four Tropical Storms, J. Coast. Res., 2008, 26–37, https://doi.org/10.2112/SI55-008.1, 2008.

Dugdale, R. C., Wilkerson, F. P., Hogue, V. E., and Marchi, A.: The role of ammonium and nitrate in spring bloom development in San Francisco Bay, Estuar. Coast. Shelf Sci., 73, 17–29, https://doi.org/10.1016/j.ecss.2006.12.008, 2007.

Elser, J. J., Bracken, M. E. S., Cleland, E. E., Gruner, D. S., Harpole, W. S., Hillebrand, H., Ngai, J. T., Seabloom, E. W., Shurin, J. B., and Smith, J. E.: Global analysis of nitrogen and phosphorus limitation of primary producers in freshwater, marine and terrestrial ecosystems, Ecol. Lett., 10, 1135–1142, https://doi.org/10.1111/j.1461-0248.2007.01113.x, 2007.

Evans, J. R. and Seemann, J. R.: The allocation of protein nitrogen in the photosynthetic apparatus: costs, consequences, and control., in: Photosynthesis, edited by: Briggs, W. R., Alan R. Liss, New York, 183–205, 1989.

Fisher, S. G., Gray, L. J., Grimm, N. B., and Busch, D. E.: Temporal Succession in a Desert Stream Ecosystem Following Flash Flooding, Ecol. Monogr., 52, 93–110, https://doi.org/10.2307/2937346, 1982.

Freeman, L. A., Corbett, D. R., Fitzgerald, A. M., Lemley, D. A., Quigg, A., and Steppe, C. N.: Impacts of Urbanization and Development on Estuarine Ecosystems and Water Quality, Estuaries Coasts, 42, 1821–1838, https://doi.org/10.1007/s12237-019-00597-z, 2019.

Gannon, J. P., Kelleher, C., and Zimmer, M.: Controls on watershed flashiness across the continental US, J. Hydrol., 609, 127713, https://doi.org/10.1016/j.jhydrol.2022.127713, 2022.

Gold, A., Thompson, S., Magel, C., and Piehler, M.: Urbanization alters coastal plain stream carbon export and dissolved oxygen dynamics, Sci. Total Environ., 747, 141132, https://doi.org/10.1016/j.scitotenv.2020.141132, 2020.

Gregory, K. J.: Wolman MG (1967) A cycle of sedimentation and erosion in urban river channels. Geografiska Annaler 49A: 385-395., Prog. Phys. Geogr., 35, 831–841, https://doi.org/10.1177/0309133311414527, 2011.

Grimm, N. B., Faeth, S. H., Golubiewski, N. E., Redman, C. L., Wu, J., Bai, X., and Briggs, J. M.: Global Change and the Ecology of Cities, Science, 319, 756–760, 2008.

Groffman, P. M., Law, N. L., Belt, K. T., Band, L. E., and Fisher, G. T.: Nitrogen Fluxes and Retention in Urban Watershed Ecosystems, Ecosystems, 7, 393–403, https://doi.org/10.1007/s10021-003-0039-x, 2004.

Guildford, S. J. and Hecky, R. E.: Total nitrogen, total phosphorus, and nutrient limitation in lakes and oceans: Is there a common relationship?, Limnol. Oceanogr., 45, 1213–1223, https://doi.org/10.4319/lo.2000.45.6.1213, 2000.

Harris, L. A., Hodgkins, C. L. S., Day, M. C., Austin, D., Testa, J. M., Boynton, W., Van Der Tak, L., and Chen, N. W.: Optimizing recovery of eutrophic estuaries: Impact of destratification and re-aeration on nutrient and dissolved oxygen dynamics, Ecol. Eng., 75, 470–483, https://doi.org/10.1016/j.ecoleng.2014.11.028, 2015.

He, Q. and Silliman, B. R.: Climate Change, Human Impacts, and Coastal Ecosystems in the Anthropocene, Curr. Biol., 29, R1021–R1035, https://doi.org/10.1016/j.cub.2019.08.042, 2019.

Hession, W. C., Pizzuto, J. E., Johnson, T. E., and Horwitz, R. J.: Influence of bank vegetation on channel morphology in rural and urban watersheds, Geology, 31, 147–150, https://doi.org/10.1130/0091-7613(2003)031<0147:IOBVOC>2.0.CO;2, 2003.

Hopkins, K. G., Morse, N. B., Bain, D. J., Bettez, N. D., Grimm, N. B., Morse, J. L., Palta, M. M., Shuster, W. D., Bratt, A. R., and Suchy, A. K.: Assessment of Regional Variation in Streamflow Responses to Urbanization and the Persistence of Physiography, Environ. Sci. Technol., 49, 2724–2732, https://doi.org/10.1021/es505389y, 2015.

Hopkinson, C. S. and Vallino, J. J.: The relationships among man's activities in watersheds and estuaries: A model of runoff effects on patterns of estuarine community metabolism, Estuaries, 18, 598–621, https://doi.org/10.2307/1352380, 1995.

Howarth, R. W.: Nutrient Limitation of Net Primary Production in Marine Ecosystems, Annu. Rev. Ecol. Syst., 19, 89–110, 1988.

Howarth, R. W. and Marino, R.: Nitrogen as the limiting nutrient for eutrophication in coastal marine ecosystems: Evolving views over three decades, Limnol. Oceanogr., 51, 364–376, https://doi.org/10.4319/lo.2006.51.1_part_2.0364, 2006.

Isbell, F., Craven, D., Connolly, J., Loreau, M., Schmid, B., Beierkuhnlein, C., Bezemer, T. M., Bonin, C., Bruelheide, H., de Luca, E., Ebeling, A., Griffin, J. N., Guo, Q., Hautier, Y., Hector, A., Jentsch, A., Kreyling, J., Lanta, V., Manning, P., Meyer, S. T., Mori, A. S., Naeem, S., Niklaus, P. A., Polley, H. W., Reich, P. B., Roscher, C., Seabloom, E. W., Smith, M. D., Thakur, M. P., Tilman, D., Tracy, B. F., van der Putten, W. H., van Ruijven, J., Weigelt, A., Weisser, W. W., Wilsey, B., and Eisenhauer, N.: Biodiversity increases the resistance of ecosystem productivity to climate extremes, Nature, 526, 574–577, https://doi.org/10.1038/nature15374, 2015.

Kannel, P. R., Lee, S., Lee, Y.-S., Kanel, S. R., and Khan, S. P.: Application of Water Quality Indices and Dissolved Oxygen as Indicators for River Water Classification and Urban Impact Assessment, Environ. Monit. Assess., 132, 93–110, https://doi.org/10.1007/s10661-006-9505-1, 2007.

Karra, K., Kontgis, C., Statman-Weil, Z., Mazzariello, J. C., Mathis, M., and Brumby, S. P.: Global land use / land cover with Sentinel 2 and deep learning, in: 2021 IEEE International Geoscience and Remote Sensing Symposium IGARSS, IGARSS 2021 - 2021 IEEE International Geoscience and Remote Sensing Symposium, Brussels, Belgium, 4704–4707, https://doi.org/10.1109/IGARSS47720.2021.9553499, 2021.

Kaushal, S. S., Likens, G. E., Pace, M. L., Utz, R. M., Haq, S., Gorman, J., and Grese, M.: Freshwater salinization syndrome on a continental scale, Proc. Natl. Acad. Sci., 115, E574–E583, https://doi.org/10.1073/pnas.1711234115, 2018.

Kemp, W. M. and Boynton, W. R.: Influence of biological and physical processes on dissolved oxygen dynamics in an estuarine system: Implications for measurement of community metabolism, Estuar. Coast. Mar. Sci., 11, 407–431, https://doi.org/10.1016/S0302-3524(80)80065-X, 1980.

Kemp, W. M., Testa, J. M., Conley, D. J., Gilbert, D., and Hagy, J. D.: Temporal responses of coastal hypoxia to nutrient loading and physical controls, Biogeosciences, 6, 2985–3008, https://doi.org/10.5194/bg-6-2985-2009, 2009.

Kornelsen, K. C. and Coulibaly, P.: Synthesis review on groundwater discharge to surface water in the Great Lakes Basin, J. Gt. Lakes Res., 40, 247–256, https://doi.org/10.1016/j.jglr.2014.03.006, 2014.

Kyzar, T., Safak, I., Cebrian, J., Clark, M. W., Dix, N., Dietz, K., Gittman, R. K., Jaeger, J., Radabaugh, K. R., Roddenberry, A., Smith, C. S., Sparks, E. L., Stone, B., Sundin, G., Taubler, M., and Angelini, C.: Challenges and opportunities for sustaining coastal wetlands and oyster reefs in the southeastern United States, J. Environ. Manage., 296, 113178, https://doi.org/10.1016/j.jenvman.2021.113178, 2021.

Lake, P. S.: Resistance, Resilience and Restoration, Ecol. Manag. Restor., 14, 20–24, https://doi.org/10.1111/emr.12016, 2013.

Leopold, L. B.: Hydrology for urban land planning - A guidebook on the hydrologic effects of urban land use, Circular, U.S. Geological Survey, https://doi.org/10.3133/cir554, 1968.

Li, C., Zwiers, F., Zhang, X., Chen, G., Lu, J., Li, G., Norris, J., Tan, Y., Sun, Y., and Liu, M.: Larger Increases in More Extreme Local Precipitation Events as Climate Warms, Geophys. Res. Lett., 46, 6885–6891, https://doi.org/10.1029/2019GL082908, 2019.

Liao, A., Han, D., Song, X., and Yang, S.: Impacts of storm events on chlorophyll-a variations and controlling factors for algal bloom in a river receiving reclaimed water, J. Environ. Manage., 297, 113376, https://doi.org/10.1016/j.jenvman.2021.113376, 2021.

Llansó, R. J.: Effects of hypoxia on estuarine benthos: the lower Rappahannock River (Chesapeake Bay), a case study, Estuar. Coast. Shelf Sci., 35, 491–515, https://doi.org/10.1016/S0272-7714(05)80027-7, 1992.

Loken, L. C., Van Nieuwenhuyse, E. E., Dahlgren, R. A., Lenoch, L. E. K., Stumpner, P. R., Burau, J. R., and Sadro, S.: Assessment of multiple ecosystem metabolism methods in an estuary, Limnol. Oceanogr. Methods, 19, 741–757, https://doi.org/10.1002/lom3.10458, 2021.

Macan, T. T.: The temperature of a small stony stream, Hydrobiologia, 12, 89–106, https://doi.org/10.1007/BF00034143, 1958.

Mallin, M. A., Johnson, V. L., and Ensign, S. H.: Comparative impacts of stormwater runoff on water quality of an urban, a suburban, and a rural stream, Environ. Monit. Assess., 159, 475–91, https://doi.org/10.1007/s10661-008-0644-4, 2009.

Martínez, M. L., Intralawan, A., Vázquez, G., Pérez-Maqueo, O., Sutton, P., and Landgrave, R.: The coasts of our world: Ecological, economic and social importance, Ecol. Econ., 63, 254–272, https://doi.org/10.1016/j.ecolecon.2006.10.022, 2007.

McCluney, K. E., Poff, N. L., Palmer, M. A., Thorp, J. H., Poole, G. C., Williams, B. S., Williams, M. R., and Baron, J. S.: Riverine macrosystems ecology: sensitivity, resistance, and resilience of whole river basins with human alterations, Front. Ecol. Environ., 12, 48–58, https://doi.org/10.1890/120367, 2014.

McSweeney, J. M., Chant, R. J., Wilkin, J. L., and Sommerfield, C. K.: Suspended-Sediment Impacts on Light-Limited Productivity in the Delaware Estuary, Estuaries Coasts, 40, 977–993, https://doi.org/10.1007/s12237-016-0200-3, 2017.

Mulholland, P. J., Fellows, C. S., Tank, J. L., Grimm, N. B., Webster, J. R., Hamilton, S. K., Martí, E., Ashkenas, L., Bowden, W. B., Dodds, W. K., Mcdowell, W. H., Paul, M. J., and Peterson, B. J.: Inter-biome comparison of factors controlling stream metabolism, Freshw. Biol., 46, 1503–1517, https://doi.org/10.1046/j.1365-2427.2001.00773.x, 2001.

Mulholland, P. J., Helton, A. M., Poole, G. C., Hall, R. O., Hamilton, S. K., Peterson, B. J., Tank, J. L., Ashkenas, L. R., Cooper, L. W., Dahm, C. N., Dodds, W. K., Findlay, S. E. G., Gregory, S. V., Grimm, N. B., Johnson, S. L., McDowell, W. H., Meyer, J. L., Valett, H. M., Webster, J. R., Arango, C. P., Beaulieu, J. J., Bernot, M. J., Burgin, A. J., Crenshaw, C. L., Johnson, L. T., Niederlehner, B. R., O'Brien, J. M., Potter, J. D., Sheibley, R. W., Sobota, D. J., and Thomas, S. M.: Stream denitrification across biomes and its response to anthropogenic nitrate loading, Nature, 452, 202–205, https://doi.org/10.1038/nature06686, 2008.

Murrell, M. C., Caffrey, J. M., Marcovich, D. T., Beck, M. W., Jarvis, B. M., and Hagy, J. D.: Seasonal oxygen dynamics in a warm temperate estuary: effects of hydrologic variability on measurements of primary production, respiration, and net metabolism, Estuaries Coasts J. Estuar. Res. Fed., 41, 690–707, https://doi.org/10.1007/s12237-017-0328-9, 2018.

NOAA National Estuarine Research Reserve System (NERRS): https://cdmo.baruch.sc.edu/, last access: 26 July 2023.

Ni, W., Li, M., and Testa, J. M.: Discerning effects of warming, sea level rise and nutrient management on long-term hypoxia trends in Chesapeake Bay, Sci. Total Environ., 737, 139717, https://doi.org/10.1016/j.scitotenv.2020.139717, 2020.

O'Dell, J. W.: Determination Of Nitrate-Nitrite Nitrogen by Automated Colorimetry, in: Methods for the Determination of Metals in Environmental Samples, Elsevier, 464–478, https://doi.org/10.1016/B978-0-8155-1398-8.50026-4, 1996a.

O'Dell, J. W.: Determination of Phosphorus by Semi-Automated Colorimetry, in: Methods for the Determination of Metals in Environmental Samples, Elsevier, 479–495, https://doi.org/10.1016/B978-0-8155-1398-8.50027-6, 1996b.

O'Driscoll, M., Clinton, S., Jefferson, A., Manda, A., and McMillan, S.: Urbanization Effects on Watershed Hydrology and In-Stream Processes in the Southern United States, Water, 2, 605–648, https://doi.org/10.3390/w2030605, 2010.

Odum, H. T.: Primary Production in Flowing Waters, Limnol. Oceanogr., 1, 102–117, https://doi.org/10.4319/lo.1956.1.2.0102, 1956.

Ombadi, M. and Varadharajan, C.: Urbanization and aridity mediate distinct salinity response to floods in rivers and streams across the contiguous United States, Water Res., 220, 118664, https://doi.org/10.1016/j.watres.2022.118664, 2022.

Orwin, K. H. and Wardle, D. A.: New indices for quantifying the resistance and resilience of soil biota to exogenous disturbances, Soil Biol. Biochem., 36, 1907–1912, https://doi.org/10.1016/j.soilbio.2004.04.036, 2004.

Paerl, H. W.: Why does N-limitation persist in the world's marine waters?, Mar. Chem., 206, 1–6, https://doi.org/10.1016/j.marchem.2018.09.001, 2018.
Paerl, H. W. and Piehler, M. F.: Chapter 11 - Nitrogen and Marine Eutrophication, in: Nitrogen in the Marine Environment (Second Edition), edited by: Capone, D. G., Bronk, D. A., Mulholland, M. R., and Carpenter, E. J., Academic Press, San Diego, 529–567, https://doi.org/10.1016/B978-0-12-372522-6.00011-6, 2008.
Parker, A. E., Hogue, V. E., Wilkerson, F. P., and Dugdale, R. C.: The effect of inorganic nitrogen speciation on primary production in the San Francisco Estuary, Estuar. Coast. Shelf Sci., 104–105, 91–101, https://doi.org/10.1016/j.ecss.2012.04.001, 2012.
Pennock, J. R. and Sharp, J. H.: Phytoplankton production in the Delaware Estuary: temporal and spatial variability, Mar. Ecol. Prog. Ser., 34, 143–155, 1986.
Pickett, S. T. A., Cadenasso, M. L., Grove, J. M., Boone, C. G., Groffman, P. M., Irwin, E., Kaushal, S. S., Marshall, V., McGrath, B. P., Nilon, C. H., Pouyat, R. V., Szlavecz, K., Troy, A., and Warren, P.: Urban ecological systems: Scientific foundations and a decade of progress, J. Environ. Manage., 92, 331–362, https://doi.org/10.1016/j.jenvman.2010.08.022, 2011.
Pimm, S. L.: The complexity and stability of ecosystems, Nature, 307, 321–326, https://doi.org/10.1038/307321a0, 1984.
Poff, N. L., Bledsoe, B. P., and Cuhaciyan, C. O.: Hydrologic variation with land use across the contiguous United States: Geomorphic and ecological consequences for stream ecosystems, Geomorphology, 79, 264–285, https://doi.org/10.1016/j.geomorph.2006.06.032, 2006.
QGIS Geographic Information System: https://www.qgis.org/en/site/, last access: 30 January 2024.
Rabalais, N. N., Díaz, R. J., Levin, L. A., Turner, R. E., Gilbert, D., and Zhang, J.: Dynamics and distribution of natural and human-caused hypoxia, Biogeosciences, 7, 585–619, https://doi.org/10.5194/bg-7-585-2010, 2010.
Raimonet, M. and Cloern, J. E.: Estuary–ocean connectivity: fast physics, slow biology, Glob. Change Biol., 23, 2345–2357, https://doi.org/10.1111/gcb.13546, 2017.
Raymond, P. A. and Cole, J. J.: Gas exchange in rivers and estuaries: Choosing a gas transfer velocity, Estuaries, 24, 312–317, https://doi.org/10.2307/1352954, 2001.
Raymond, P. A., Zappa, C. J., Butman, D., Bott, T. L., Potter, J., Mulholland, P., Laursen, A. E., McDowell, W. H., and Newbold, D.: Scaling the gas transfer velocity and hydraulic geometry in streams and small rivers: Gas transfer velocity and hydraulic geometry, Limnol. Oceanogr. Fluids Environ., 2, 41–53, https://doi.org/10.1215/21573689-1597669, 2012.
Redfield, A. C.: On the Properties of Organic Derivatives in Sea Water and Their Relation to Composition of the Phytoplankton, in: James Johnstone Memorial Volume, University Press of Liverpool, 176–192, 1934.
Reisinger, A. J., Groffman, P. M., and Rosi-Marshall, E. J.: Nitrogen-cycling process rates across urban ecosystems, FEMS Microbiol. Ecol., 92, fiw198, https://doi.org/10.1093/femsec/fiw198, 2016.
Reisinger, A. J., Rosi, E. J., Bechtold, H. A., Doody, T. R., Kaushal, S. S., and Groffman, P. M.: Recovery and resilience of urban stream metabolism following Superstorm Sandy and other floods, Ecosphere, 8, e01776, https://doi.org/10.1002/ecs2.1776, 2017.
Schindler, D. W.: Evolution of Phosphorus Limitation in Lakes, Science, 195, 260–262, https://doi.org/10.1126/science.195.4275.260, 1977.
Scully, M. E.: Wind Modulation of Dissolved Oxygen in Chesapeake Bay, Estuaries Coasts, 33, 1164–1175, https://doi.org/10.1007/s12237-010-9319-9, 2010.
Simon, A. and Rinaldi, M.: Disturbance, stream incision, and channel evolution: The roles of excess transport capacity and boundary materials in controlling channel response, Geomorphology, 79, 361–383, https://doi.org/10.1016/j.geomorph.2006.06.037, 2006.
Smith, S. V.: Phosphorus versus nitrogen limitation in the marine environment, Limnol. Oceanogr., 29, 1149–1160, https://doi.org/10.4319/lo.1984.29.6.1149, 1984.
Song, C., Dodds, W. K., Rüegg, J., Argerich, A., Baker, C. L., Bowden, W. B., Douglas, M. M., Farrell, K. J., Flinn, M. B., Garcia, E. A., Helton, A. M., Harms, T. K., Jia, S., Jones, J. B., Koenig, L. E.,

Kominoski, J. S., McDowell, W. H., McMaster, D., Parker, S. P., Rosemond, A. D., Ruffing, C. M., Sheehan, K. R., Trentman, M. T., Whiles, M. R., Wollheim, W. M., and Ballantyne, F.: Continental-scale decrease in net primary productivity in streams due to climate warming, Nat. Geosci., 11, 415–420, https://doi.org/10.1038/s41561-018-0125-5, 2018.

Thayne, M. W., Kraemer, B. M., Mesman, J. P., Ibelings, B. W., and Adrian, R.: Antecedent lake conditions shape resistance and resilience of a shallow lake ecosystem following extreme wind storms, Limnol. Oceanogr., 67, S101–S120, https://doi.org/10.1002/lno.11859, 2022.

Thayne, M. W., Kraemer, B. M., Mesman, J. P., Pierson, D., Laas, A., de Eyto, E., Ibelings, B. W., and Adrian, R.: Lake surface water temperature and oxygen saturation resistance and resilience following extreme storms: chlorophyll a shapes resistance to storms, Inland Waters, 13, 339–361, https://doi.org/10.1080/20442041.2023.2242081, 2023.

Tsai, J.-W., Kratz, T. K., Hanson, P. C., Kimura, N., Liu, W.-C., Lin, F.-P., Chou, H.-M., Wu, J.-T., and Chiu, C.-Y.: Metabolic changes and the resistance and resilience of a subtropical heterotrophic lake to typhoon disturbance, Can. J. Fish. Aquat. Sci., 68, 768–780, https://doi.org/10.1139/f2011-024, 2011.

Uehlinger, U.: Resistance and resilience of ecosystem metabolism in a flood-prone river system, Freshw. Biol., 45, 319–332, https://doi.org/10.1111/j.1365-2427.2000.00620.x, 2000.

U.S. EPA.: Method 350.1: Nitrogen, Ammonia (Calorimetric, Automated Phenate), 1993a.

U.S. EPA.: Method 446.0: In Vitro Determination of Chlorophylls a, b, c1+c2 and Pheopigments in Marine and Freshwater Algae by Visible Spectrophotometry, 1993b.

Utz, R. M., Hopkins, K. G., Beesley, L., Booth, D. B., Hawley, R. J., Baker, M. E., Freeman, M. C., and L. Jones, K.: Ecological resistance in urban streams: the role of natural and legacy attributes, Freshw. Sci., 35, 380–397, https://doi.org/10.1086/684839, 2016.

Van Meerbeek, K., Jucker, T., and Svenning, J.-C.: Unifying the concepts of stability and resilience in ecology, J. Ecol., 109, 3114–3132, https://doi.org/10.1111/1365-2745.13651, 2021.

Vietz, G. J., Walsh, C. J., and Fletcher, T. D.: Urban hydrogeomorphology and the urban stream syndrome: Treating the symptoms and causes of geomorphic change, Prog. Phys. Geogr. Earth Environ., 40, 480–492, https://doi.org/10.1177/0309133315605048, 2016.

Vitousek, P. M. and Howarth, R. W.: Nitrogen limitation on land and in the sea: How can it occur?, Biogeochemistry, 13, 87–115, https://doi.org/10.1007/BF00002772, 1991.

Walsh, C. J., Roy, A. H., Feminella, J. W., Cottingham, P. D., Groffman, P. M., and Morgan, R. P.: The urban stream syndrome: current knowledge and the search for a cure, J. North Am. Benthol. Soc., 24, 706–723, https://doi.org/10.1899/04-028.1, 2005.

Wetz, M. S. and Yoskowitz, D. W.: An ‘extreme’ future for estuaries? Effects of extreme climatic events on estuarine water quality and ecology, Mar. Pollut. Bull., 69, 7–18, https://doi.org/10.1016/j.marpolbul.2013.01.020, 2013.

Zahn, E., Welty, C., Smith, J. A., Kemp, S. J., Baeck, M.-L., and Bou-Zeid, E.: The Hydrological Urban Heat Island: Determinants of Acute and Chronic Heat Stress in Urban Streams, JAWRA J. Am. Water Resour. Assoc., 57, 941–955, https://doi.org/10.1111/1752-1688.12963, 2021.

Zarnetske, J. P., Haggerty, R., Wondzell, S. M., Bokil, V. A., and González-Pinzón, R.: Coupled transport and reaction kinetics control the nitrate source-sink function of hyporheic zones, Water Resour. Res., 48, https://doi.org/10.1029/2012WR011894, 2012.

Zhang, J., Gilbert, D., Gooday, A. J., Levin, L., Naqvi, S. W. A., Middelburg, J. J., Scranton, M., Ekau, W., Peña, A., Dewitte, B., Oguz, T., Monteiro, P. M. S., Urban, E., Rabalais, N. N., Ittekkot, V., Kemp, W. M., Ulloa, O., Elmgren, R., Escobar-Briones, E., and Van der Plas, A. K.: Natural and human-induced hypoxia and consequences for coastal areas: synthesis and future development, Biogeosciences, 7, 1443–1467, https://doi.org/10.5194/bg-7-1443-2010, 2010.

Zhang, M., Krom, M. D., Lin, J., Cheng, P., and Chen, N.: Effects of a Storm on the Transformation and Export of Phosphorus Through a Subtropical River-Turbid Estuary Continuum Revealed by Continuous Observation, J. Geophys. Res. Biogeosciences, 127, e2022JG006786, https://doi.org/10.1029/2022JG006786, 2022.

Zhang, Q., Fisher, T. R., Trentacoste, E. M., Buchanan, C., Gustafson, A. B., Karrh, R., Murphy, R. R.,

Keisman, J., Wu, C., Tian, R., Testa, J. M., and Tango, P. J.: Nutrient limitation of phytoplankton in Chesapeake Bay: Development of an empirical approach for water-quality management, Water Res., 188, 116407, https://doi.org/10.1016/j.watres.2020.116407, 2021.
Zheng, Y., Huang, J., Feng, Y., Xue, H., Xie, X., Tian, H., Yao, Y., Luo, L., Guo, X., and Liu, Y.: The Effects of Seasonal Wind Regimes on the Evolution of Hypoxia in Chesapeake Bay: Results from A Terrestrial-Estuarine-Ocean Biogeochemical Modeling System, Prog. Oceanogr., 103207, https://doi.org/10.1016/j.pocean.2024.103207, 2024.
Zhi, W., Feng, D., Tsai, W.-P., Sterle, G., Harpold, A., Shen, C., and Li, L.: From Hydrometeorology to River Water Quality: Can a Deep Learning Model Predict Dissolved Oxygen at the Continental Scale?, Environ. Sci. Technol., 55, 2357–2368, https://doi.org/10.1021/acs.est.0c06783, 2021.

Supplementary Tables.

Table S1: Multiparameter sonde position within the water column at five National Estuarine Research Reserve Systems (NERRS).

Estuary	**Monitoring location**	**Sonde position above sediment bed (m)**
Lake Superior (LKS)	Barker's Island (BA)	0.5
	Pokegama Bay (PO)	0.25
	Blatnik Bridge (BL)	5.5
	Oliver Bridge (OL)	6.5
Chesapeake Bay, Maryland (CBM)	Iron Pot Landing (IP)	0.25
	Railroad Bridge (RR)	0.25
	Mataponi Creek (MC)	0.25
Weeks Bay (WKB)	Magnolia River (MR)	0.5
	Middle Bay (MB)	0.5
	Weeks Bay (WB)	0.5
	Fish River (FR)	0.5
Guana Tolomato-Matanzas (GTM)	San Sebastian (SS)	1.0
	Pine Island (PI)	1.0
	Pellicer Creek (PC)	1.0

	Fort Matanzas (FM)	1.0
San Francisco Bay (SFB)	First Mallard (FM)	0.25 - 0.5
	Second Mallard (SM)	0.25 - 0.5
	Gallinas Creek (GC)	0.25 - 0.5
	China Camp (CC)	0.25 - 0.5

Table S2. Datetime and threshold values for major precipitation events, and breakdown of the number of events during wet and dry years at each National Estuarine Research Reserve (NERR) station.

NERR Station	**Datetime** used to select dissolved oxygen and precipitation measurements to calculate the resistance index		**Precip. event (mm)**	**Wet/Dry year**	**precip. threshold (mm/day)**
	Prior to disturbance (C_0)	**During and post disturbance (P_0)**			
Lake Superior, WI (LKS)	2017/06/24 00:00:00 -2017/06/27 23:45:00 2017/07/30 00:00:00 -2017/08/02 23:45:00 2017/08/23 00:00:00 -2017/08/25 23:45:00 2017/09/29 00:00:00 -2017/10/01 23:45:00	2017/06/28 06:00:00 -2017/06/29 23:45:00 2017/08/03 00:00:00 -2017/08/04 23:45:00 2017/08/26 00:00:00 -2017/08/28 23:45:00 2017/10/02 00:00:00 -2017/10/05 23:45:00	34.4 38.1 61.0 44.2	Wet (4)	> 25
	2020/07/14 00:00:00 -2020/07/17 23:45:00 2020/07/14 00:00:00 -2020/07/17 23:45:00 2020/08/04 00:00:00 -2020/08/06 23:45:00	2020/07/18 00:00:00 -2020/07/19 23:45:00 2020/07/21 00:00:00 -2020/07/23 23:45:00 2020/08/07 12:00:00 -2020/08/11 23:45:00	42.9 29.6 74.9	Dry (3)	
Chesapeake Bay, MD (CBM)	2018/05/10 00:00:00 -2018/05/11 12:00:00 2018/05/24 00:00:00 -2018/05/26 23:45:00 2018/05/24 00:00:00 -2018/05/26 23:45:00 2018/06/16 00:00:00 -2018/06/18 23:45:00 2018/07/13 00:00:00 -2018/07/16 23:45:00 2018/09/04 00:00:00 -2018/09/06 23:45:00 2018/09/13 00:00:00 -2018/09/15 23:45:00	2018/05/16 00:00:00 -2018/05/21 23:45:00 2018/05/27 15:00:00 -2018/05/28 23:45:00 2018/06/03 06:00:00 -2018/06/07 23:45:00 2018/06/19 12:00:00 -2018/06/25 23:45:00 2018/07/21 12:00:00 -2018/07/27 23:45:00 2018/09/09 00:00:00 -2018/09/10 23:45:00 2018/09/23 00:00:00 -2018/09/25 23:45:00	117.1 40.2 56.2 41.8 218.1 49.1 58.6	Wet (7)	>25
	2016/06/24 00:00:00 -2016/06/27 23:45:00 2016/09/15 00:00:00 -2016/09/18 23:45:00 2016/09/23 00:00:00 -2016/09/25 23:45:00	2016/07/01 12:00:00 -2016/07/02 23:45:00 2016/09/19 00:00:00 -2016/09/19 23:45:00 2016/09/28 00:00:00 -2016/09/30 23:45:00	41.0 25.2 76.4	Dry (3)	
Guana Tolomato	2017/08/19 00:00:00 -2017/08/22 23:45:00 2017/08/19 00:00:00 -2017/08/22 23:45:00	2017/09/10 00:00:00 -2017/09/21 23:45:00 2017/09/30 00:00:00 -2017/10/13 23:45:00	222.9 270.7	Wet (3)	*

Matanzas, FL (GTM)	2017/11/15 00:00:00 -2017/11/22 23:45:00	2017/11/23 00:00:00 -2017/11/25 23:45:00	123.1		
	2016/06/01 00:00:00 -2016/06/04 23:45:00	2016/06/05 12:00:00 -2016/06/07 23:45:00	127.9	Dry (4)	
	2016/08/21 00:00:00 -2016/08/27 23:45:00	2016/08/28 00:00:00 -2016/09/06 23:45:00	67.2		
	2016/09/05 00:00:00 -2016/09/08 23:45:00	2016/09/14 00:00:00 -2016/09/19 23:45:00	27.3		
	2016/09/21 00:00:00 -2016/09/25 23:45:00	2016/09/28 00:00:00 -2016/10/17 23:45:00	193.3		
Weeks Bay, AL (WKB)	2018/05/19 00:00:00 -2018/05/22 23:45:00	2018/05/23 00:00:00 -2018/05/27 23:45:00	90.9	Wet (8)	> 30
	2018/06/07 00:00:00 -2018/06/09 23:45:00	2018/06/11 00:00:00 -2018/06/13 23:45:00	47.0		
	2018/06/28 00:00:00 -2018/06/30 23:45:00	2018/07/01 12:00:00 -2018/07/09 23:45:00	86.3		
	2018/07/12 00:00:00 -2018/07/14 23:45:00	2018/07/16 09:00:00 -2018/07/18 23:45:00	53.7		
	2018/08/25 00:00:00 -2018/08/26 23:45:00	2018/09/01 00:00:00 -2018/09/03 23:45:00	56.6		
	2018/08/25 00:00:00 -2018/08/26 23:45:00	2018/09/04 00:00:00 -2018/09/08 23:45:00	128.6		
	2018/09/19 00:00:00 -2018/09/20 23:45:00	2018/09/21 12:00:00 -2018/09/23 23:45:00	46.7		
	2018/09/19 00:00:00 -2018/09/20 23:45:00	2018/09/24 00:00:00 -2018/09/29 23:45:00	66.5		
	2019/04/01 00:00:00 -2019/04/03 23:45:00	2019/04/04 09:00:00 -2019/04/04 23:45:00	40.0	Dry (7)	
	2019/04/15 00:00:00 -2019/04/17 23:45:00	**2019/04/26 15:00:00 -2019/04/28 23:45:00	32.9		
	2019/06/01 00:00:00 -2019/06/04 23:45:00	2019/06/06 00:00:00 -2019/06/13 23:45:00	116.1		
	2019/06/20 00:00:00 -2019/06/25 23:45:00	2019/07/13 00:00:00 -2019/07/15 23:45:00	89.1		
	2019/08/07 00:00:00 -2019/08/10 23:45:00	2019/08/15 12:00:00 -2019/08/16 23:45:00	37.0		
	2019/08/22 00:00:00 -2019/08/24 23:45:00	2019/08/26 06:00:00 -2019/08/27 06:00:00	48.2		
	2019/10/21 00:00:00 -2019/10/24 23:45:00	2019/10/30 00:00:00 -2019/11/01 23:45:00	61.8		
San Francisco Bay, CA (SFB)	2017/01/01 00:00:00 -2017/01/02 06:00:00	2017/01/03 00:00:00 -2017/01/06 00:00:00	38.7	Wet (5)	> 20
	2017/01/01 00:00:00 -2017/01/02 06:00:00	2017/01/07 00:00:00 -2017/01/12 23:45:00	126.4		
	2017/01/01 00:00:00 -2017/01/02 06:00:00	2017/01/18 00:00:00 -2017/01/25 00:00:00	110.8		
	2017/03/11 00:00:00 -2017/03/17 23:45:00	2017/03/20 00:00:00 -2017/03/23 23:45:00	43.0		
	2017/04/01 00:00:00 -2017/04/05 06:00:00	2017/04/06 20:00:00 -2017/04/07 23:45:00	37.0		
	2018/01/06 00:00:00 -2018/01/07 23:45:00	2018/01/08 00:00:00 -2018/01/09 23:45:00	73.6	Dry (3)	
	2018/02/20 00:00:00 -2018/02/23 23:45:00	***2018/03/01 00:00:00 -2018/03/01 23:45:00	30.7		
	2018/04/04 12:00:00 -2018/04/05 12:00:00	2018/04/06 00:00:00 -2018/04/07 23:45:00	54.6		

***** For GTM 2016 the selected events were: Colin, Julia, Hermine, and Matthew. For 2017 the events were Irma and two Nor'easters.

** This resistance calculation does not include dissolved oxygen measurements during the actual rain event from 2019/04/25 only dissolved oxygen after the event, because data during the event is missing from MB monitoring location.

*** Dissolved oxygen data for the SM site is missing. No resistance was calculated for SM during that time.

Table S3: Average pre-disturbance (C_0) and post-disturbance (P_0) dissolved oxygen (mg L^{-1}) and the resistance index values for each major precipitation event across all monitoring locations at five estuaries. (.csv file)

Table S4: Resulting statistical parameters for linear regression analysis conducted for low- and high-salinity groups and on continental scale for five estuaries (this table accompanies Fig. 3).

Predictor variables regressed against mean resistance index values	Linear regression parameters: Coefficient of determination (R^2) Significance value (p)		
	Low salinity group	High-salinity group	Continental-scale
Turbidity (NTU)	$R^2 = 0.00$ $p = 0.933$	**$R^2 = 0.29$** **$p < 0.0001$**	**$R^2 = 0.06$** **$p = 0.0015$**
Salinity (ppt)	**$R^2 = 0.214$** **$p < 0.0001$**	$R^2 = 0.01$ $p = 0.495$	$R^2 = 0.001$ $p = 0.513$
Water temperature (C)	**$R^2 = 0.30$** **$p < 0.0001$**	**$R^2 = 0.59$** **$p < 0.0001$**	**$R^2 = 0.39$** **$p < 0.0001$**
Water depth (m)	**$R^2 = 0.1$** **$p < 0.0001$**	$R^2 = 0.00$ $p = 0.997$	**$R^2 = 0.10$** **$p < 0.0001$**
log(DIN) (mg L^{-1})	$R^2 = 0.05$ $p = 0.268$	**$R^2 = 0.55$** **$p = 0.004$**	**$R^2 = 0.12$** **$p = 0.031$**
PO_4^{-3} (mg L^{-1})	$R^2 = 0.03$ $p = 0.416$	$R^2 = 0.06$ $p = 0.31$	$R^2 = 0.07$ $p = 0.134$
N:P	$R^2 = 0.14$ $p = 0.077$	**$R^2 = 0.81$** **$p < 0.0001$**	$R^2 = 0.08$ $p = 0.101$
Chl-*a* (µg L^{-1})	**$R^2 = 0.46$** **$p = 0.0002$**	**$R^2 = 0.32$** **$p = 0.044$**	**$R^2 = 0.39$** **$p < 0.0001$**
Trees (%)	$R^2 = 0.01$ $p = 0.72$	**$R^2 = 0.46$** **$p = 0.011$**	$R^2 = 0.03$ $p = 0.30$

Crops (%)	$R^2 = 0.14$ $p = 0.07$	$R^2 = 0.05$ $p = 0.48$	$R^2 = 0.04$ $p = 0.22$
Built area (%)	$R^2 = 0.03$ $p = 0.41$	**$R^2 = 0.73$** **$p = 0.0002$**	**$R^2 = 0.14$** **$p = 0.02$**
Population density (ppl km^{-2})	$R^2 = 0.16$ $p = 0.051$	**$R^2 = 0.73$** **$p = 0.0002$**	**$R^2 = 0.27$** **$p = 0.001$**

Note: Significant correlations (i.e., $p < 0.05$) are shown in bold.

Supplementary figures.

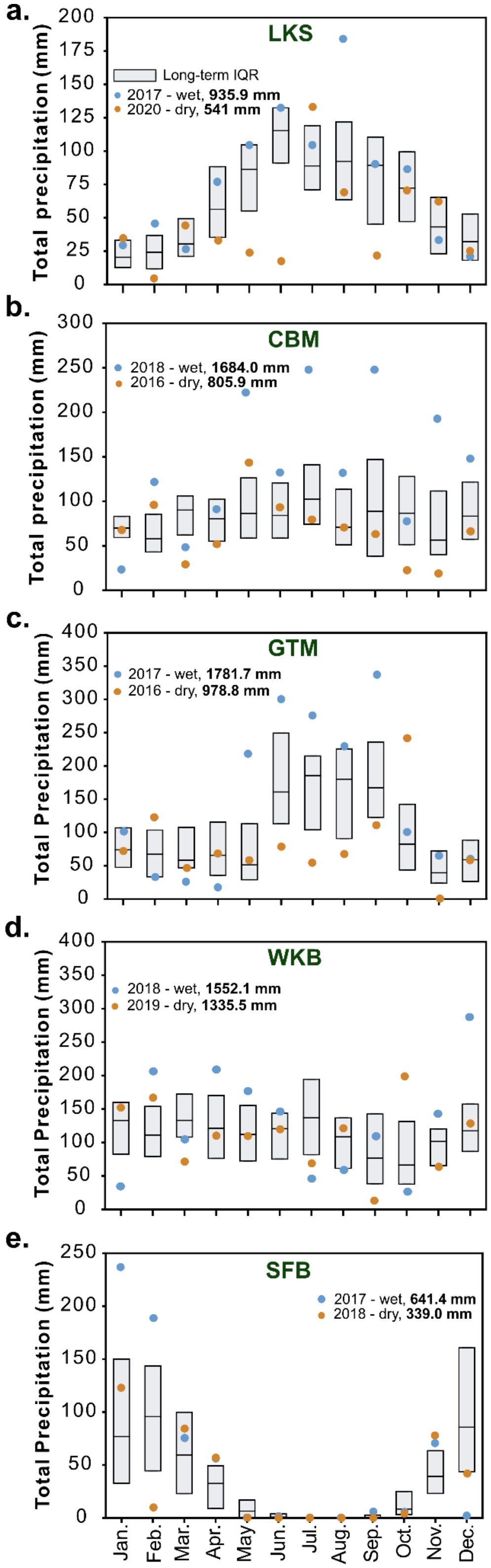

Fig. S1. Long-term (30-year) interquartile range and monthly precipitation during relatively wet and dry years. Long term precipitation data obtained from airports located in the vicinity of each selected estuarine station. a) Precipitation records from Duluth International airport were used to infer wet/dry years at Lake Superior (LKS) station. b) Washington Reagan International Airport precipitation records were used for Chesapeake Bay (CBM) station. c) Jacksonville International Airport precipitation record was used for Guana Tolomato Matanzas (GTM) station. d) Birmingham Airport precipitation records were used for Weeks Bay (WKS) station. e) San Francisco International Airport precipitation records were used for San Francisco Bay (SFB) station.

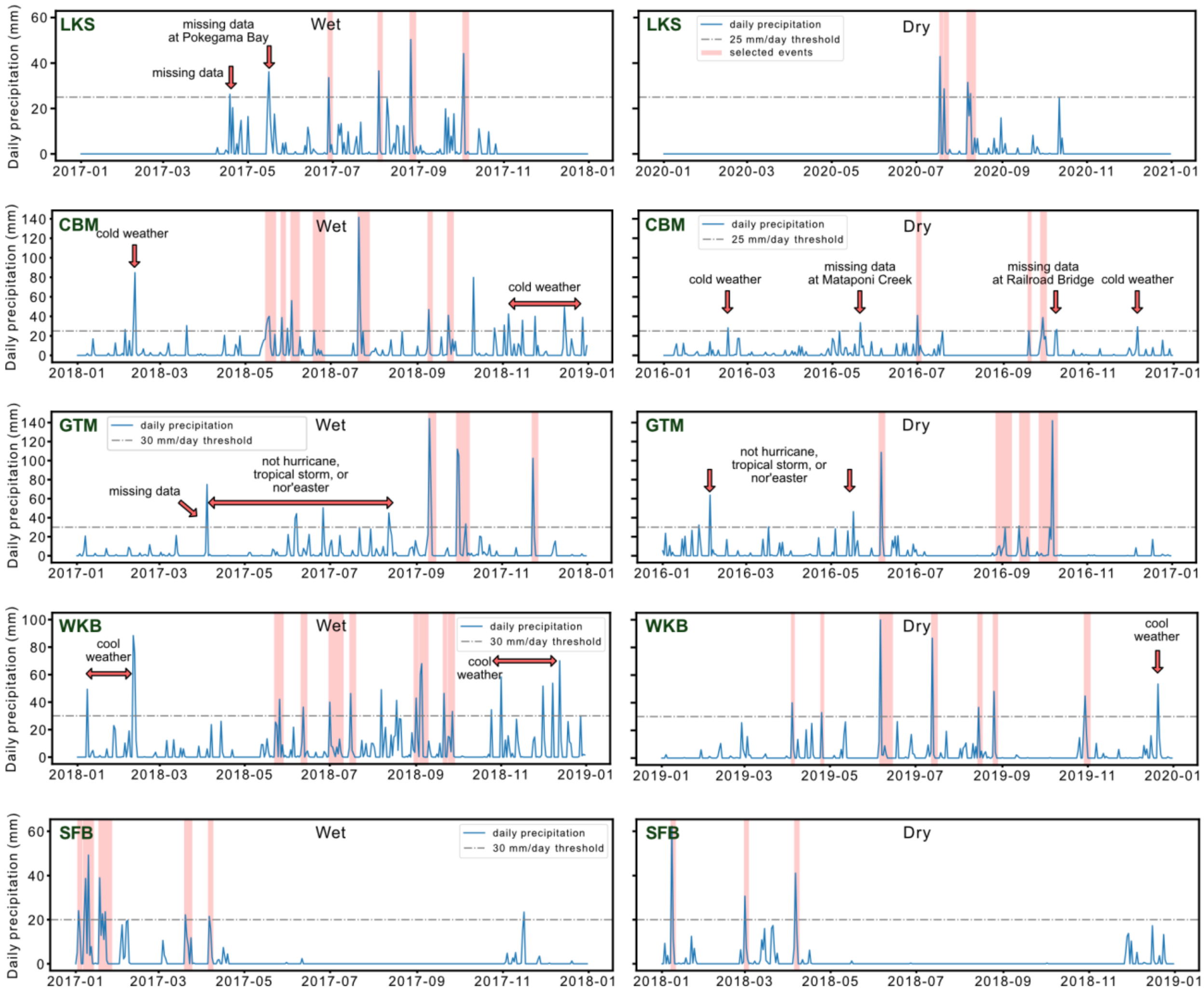

Fig. S2. Major precipitation events for each estuary during selected wet and dry years. The major precipitation events (sharded in red) identified by plotting National Estuarine Research Reserve (NERR) precipitation data collected at each estuary. The events were down-selected based on water quality data availability for each estuary, within warmer seasons, and if the event was noted in NERR metadata sheets and/or reported as hurricane, tropical storm, or nor'easter. Estuary abbreviations: Lake Superior (LKS) NERR, Chesapeake Bay, Maryland (CBM) NERR, Guana Tolomato Matanzas (GTM) NERR, Weeks Bay (WKB) NERR, and San Francisco Bay (SFB) NERR. For details about events used for resistance index calculations, please see Table S2.

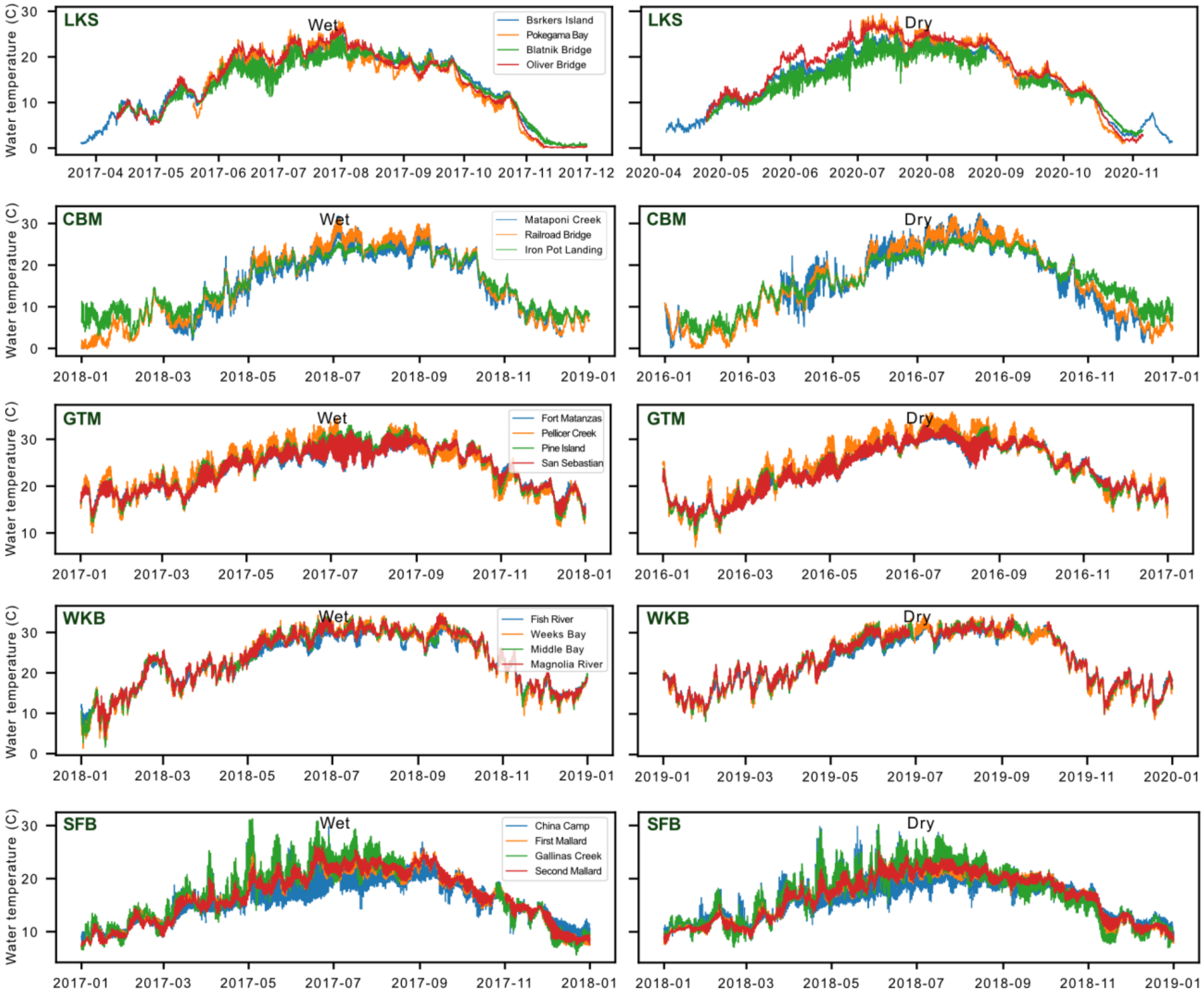

Fig. S3. Water temperature during selected wet and dry years for five National Estuarine Research Reserve (NERR) estuaries. Estuary abbreviations: Lake Superior (LKS) NERR, Chesapeake Bay, Maryland (CBM) NERR, Guana Tolomato Matanzas (GTM) NERR, Weeks Bay (WKB) NERR, and San Francisco Bay (SFB) NERR. Note: At LKS, the water temperature record extends from April to December for 2017, and from April to November for 2020 because the St. Louis River freezes over and no measurements are collected.

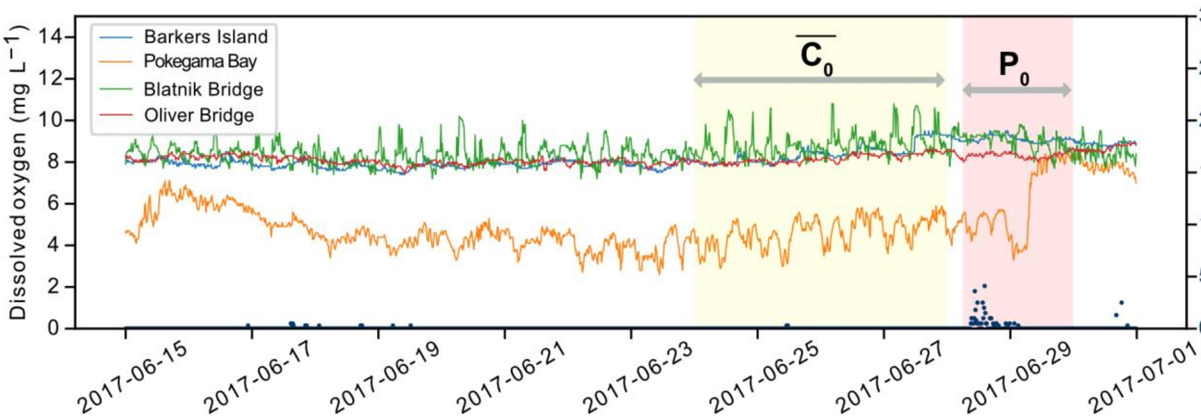

Fig. S4. Example for visualizing the selection of variables for resistance index calculations. Dissolved oxygen concentrations and precipitation at Lake Superior (LKS) NERR prior to and during a precipitation event on 06-28-2017. Yellow shaded box indicates the time used to calculate average pre-disturbance dissolved oxygen concentration (average C_0). Red shaded box indicated the time used to identify dissolved oxygen concentration post-disturbance (P_0). P_0 was identified as the maximum displacement from average C_0.

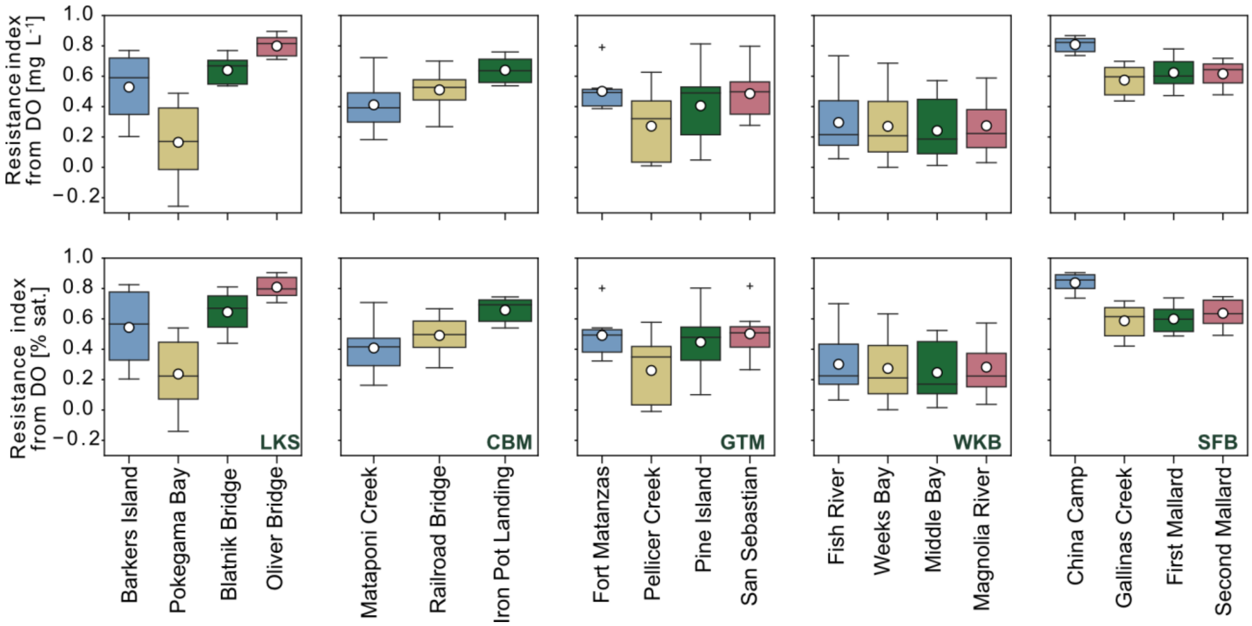

Fig. S5. Resistance index at each site calculated using dissolved oxygen (DO) concentration and DO percent saturation. (top row) Resistance index calculated using DO mg L^{-1}. (bottom row) Resistance index calculated using DO % saturation.

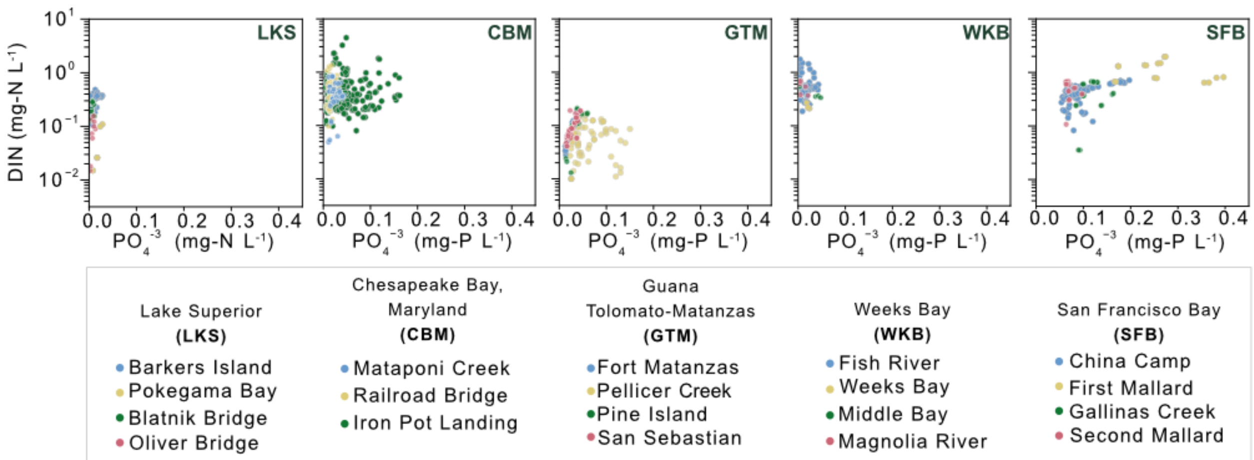

Fig. S6. Dissolved inorganic nutrient concentrations at each estuary. Dissolved inorganic nitrogen (DIN) (i.e., NO_3^- + NO_2^- + NH_4^+). Estuary abbreviations: Lake Superior (LKS) NERR, Chesapeake Bay, Maryland (CBM) NERR, Guana Tolomato Matanzas (GTM) NERR, Weeks Bay (WKB) NERR, and San Francisco Bay (SFB) NERR. For LKS estuary, the NH_4^+ measurements for dry year (2020) were missing at all monitoring locations. For WKB, the PO_4^{3-} measurements for wet year (2018) were missing at WB, MB, and MR monitoring locations.

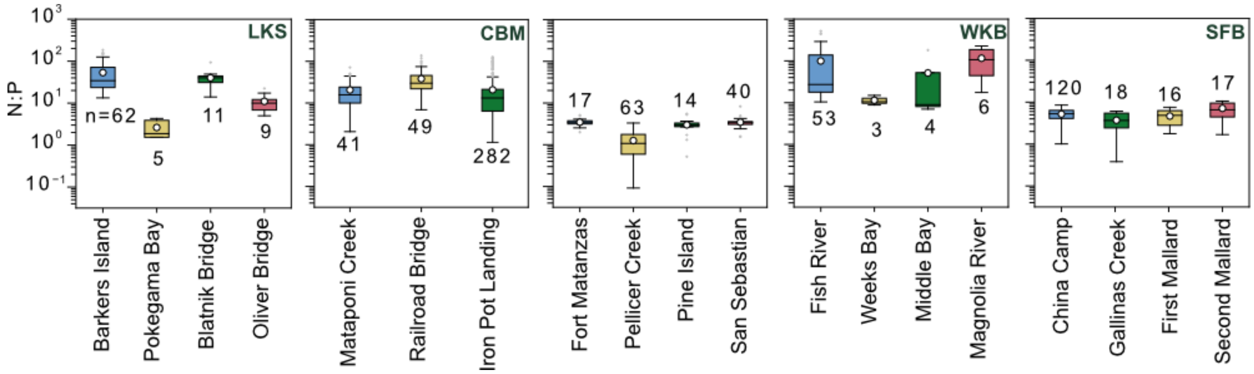

Fig. S7. Distribution of nitrogen to phosphorus ratio (N:P) within individual estuaries. Estuary abbreviations: Lake Superior (LKS) NERR, Chesapeake Bay, Maryland (CBM) NERR, Guana Tolomato Matanzas (GTM) NERR, Weeks Bay (WKB) NERR, and San Francisco Bay (SFB) NERR. Means are shown in white circles, and medians are shown in black solid lines. Boxes show the quartiles of the dataset and the whiskers show the rest of the distribution. The stoichiometric N:P was calculated using dissolved inorganic nitrogen species (i.e., NO_3^- + NO_2^- + NH_4^+) and phosphate. We note that because of missing measurements for PO_4^{-3} during the wet year at WKB- WB, MB, and MR – the N:P at these locations were calculated only for the dry year.

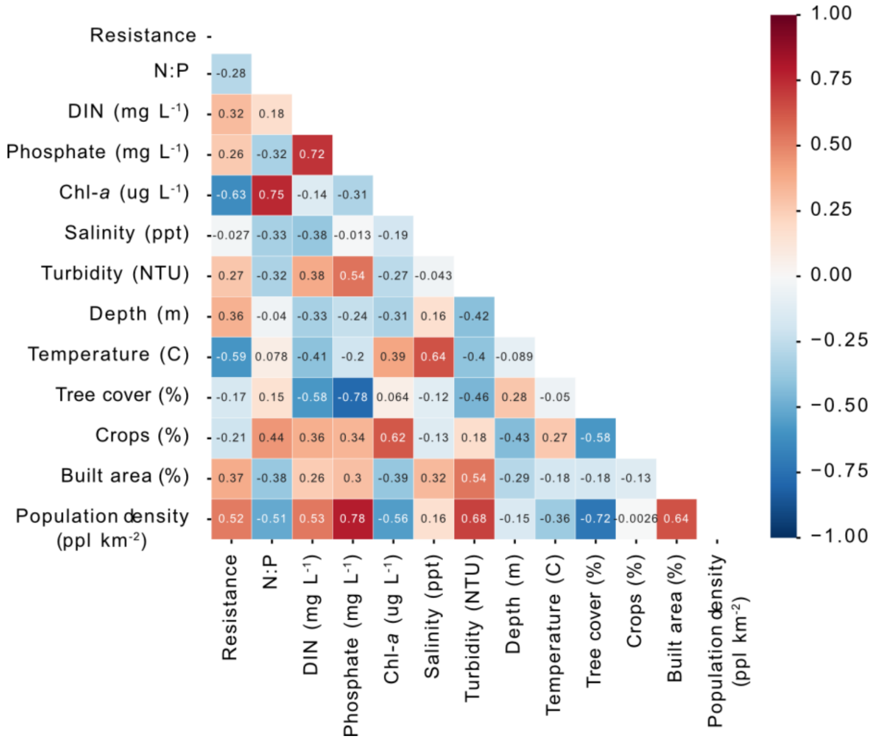

Fig. S8. Correlation matrix for resistance, water quality parameters, and land use/land cover across combined estuaries.

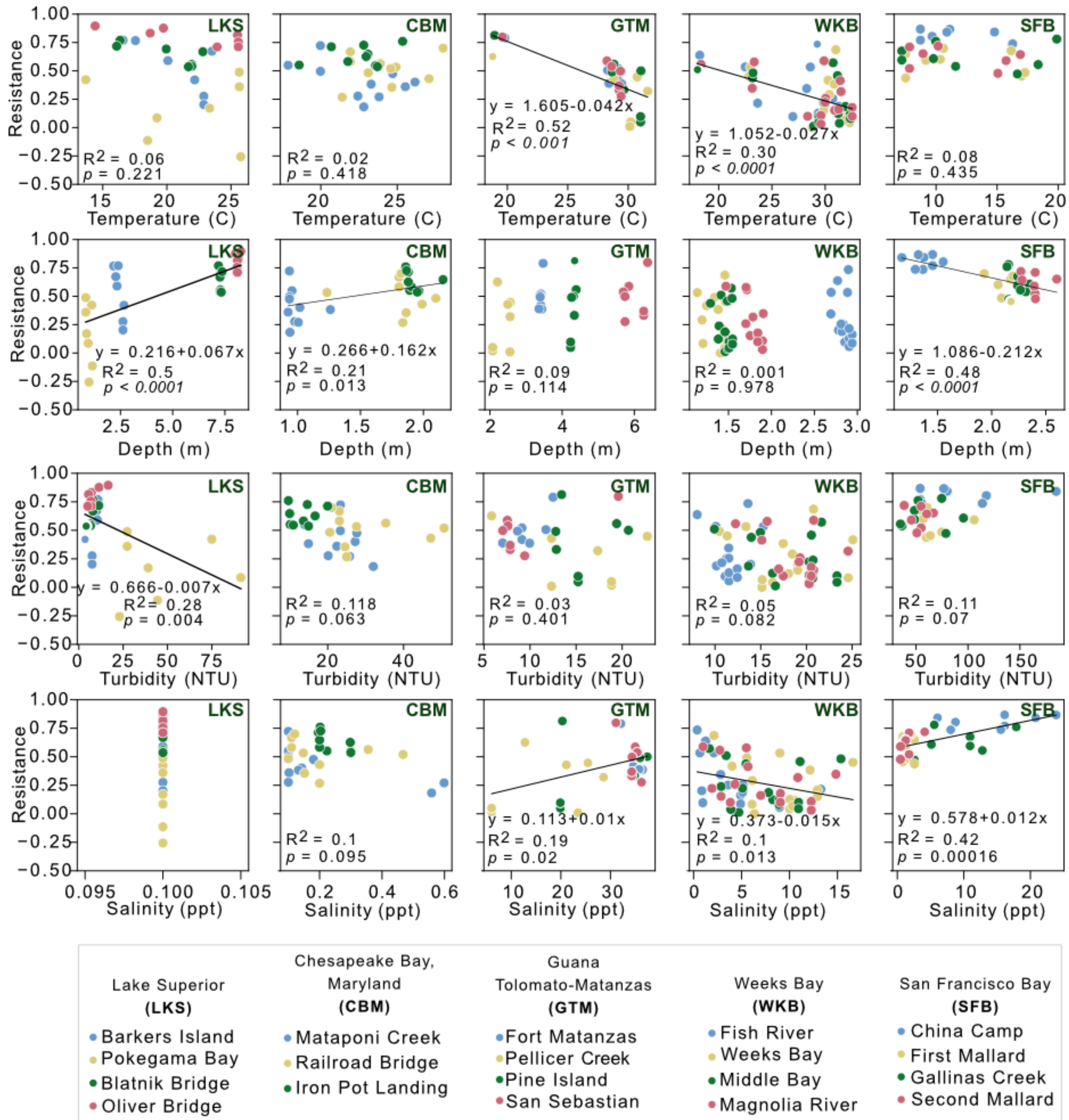

Fig. S9. Relationships of resistance to water temperature, water column depth, turbidity, and salinity at each estuary. Estuary abbreviations: Lake Superior (LKS) NERR, Chesapeake Bay, Maryland (CBM) NERR, Guana Tolomato Matanzas (GTM) NERR, Weeks Bay (WKB) NERR, and San Francisco Bay (SFB) NERR. Significant correlations ($p < 0.05$) are shown in black lines. Relationships consider mean values of physicochemical factors in context of precipitation events used in resistance index calculations (see dates in Table S2).

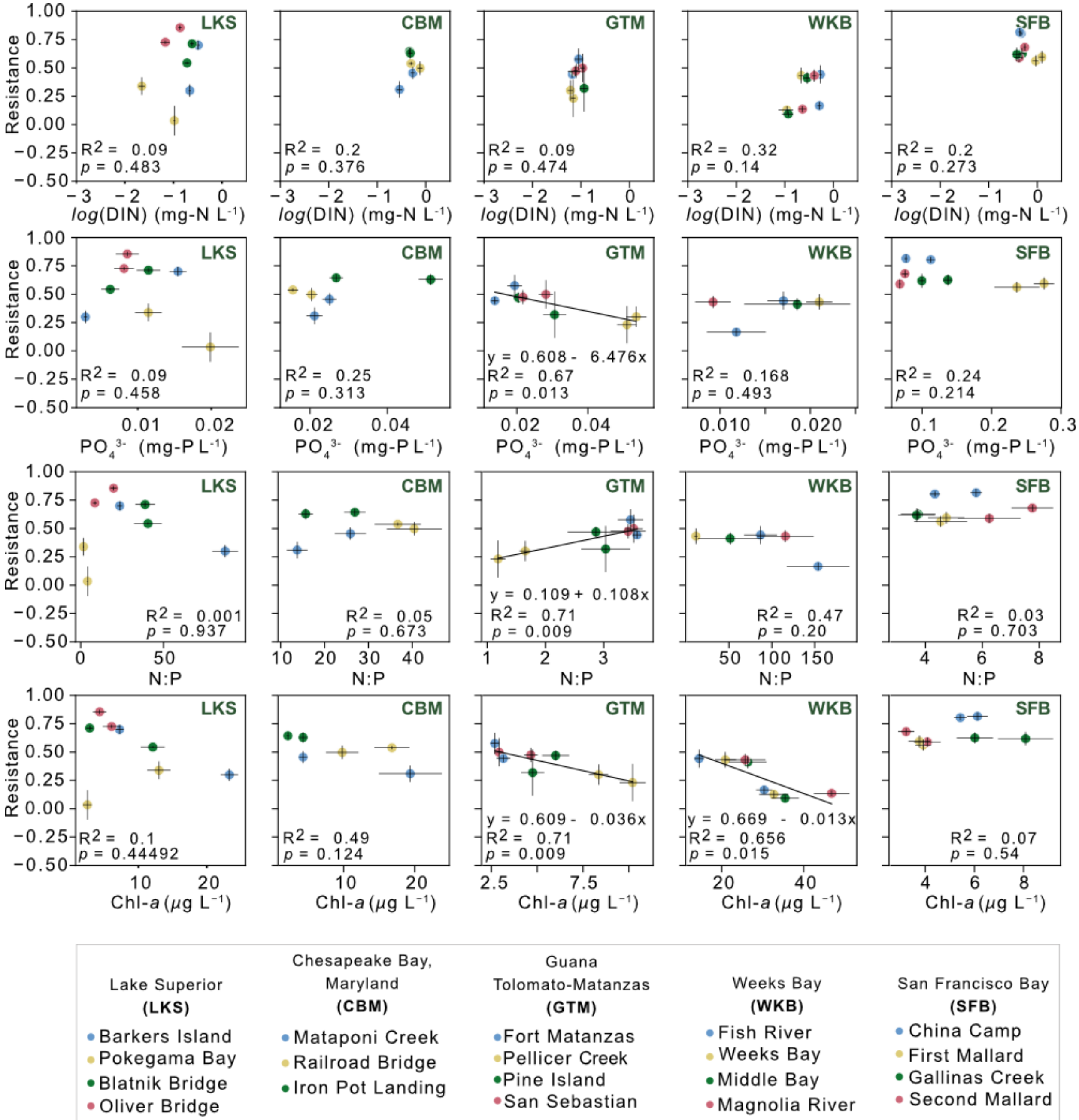

Fig. S10. Relationships of resistance to dissolved inorganic nitrogen (DIN), phosphate (PO_4^{-3}), N:P, and chlorophyll-*a* (Chl-*a*) at each estuary. Estuary abbreviations: Lake Superior (LKS) NERR, Chesapeake Bay, Maryland (CBM) NERR, Guana Tolomato Matanzas (GTM) NERR, Weeks Bay (WKB) NERR, and San Francisco Bay (SFB) NERR. Significant correlations (p < 0.05) are shown in black. Standard errors of the mean are shown in horizontal and vertical black lines. Relationships consider annual mean values of resistance and annual mean values for nutrients, N:P, and Chl-*a* calculated for wet and dry years separately.

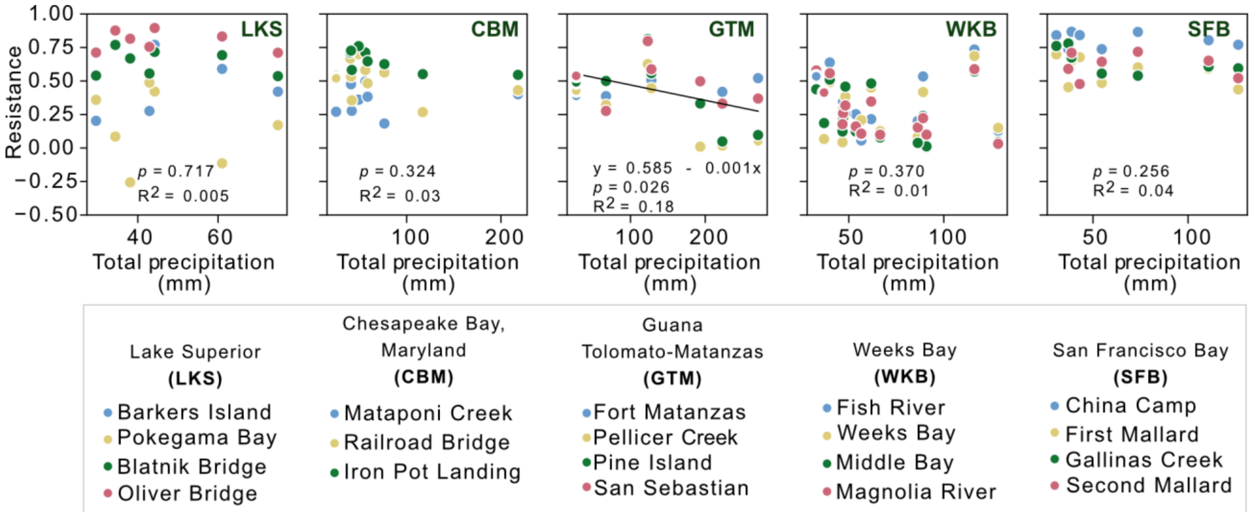

Fig. S11. Relationships between the resistance index and total precipitation during each event at each estuary. National Estuarine Reserve System (NERR) estuary abbreviations: Lake Superior (LKS) NERR, Chesapeake Bay, Maryland (CBM) NERR, Guana Tolomato Matanzas (GTM) NERR, Weeks Bay (WKB) NERR, and San Francisco Bay (SFB) NERR. Significant correlations ($p < 0.05$) are indicated with a black line.

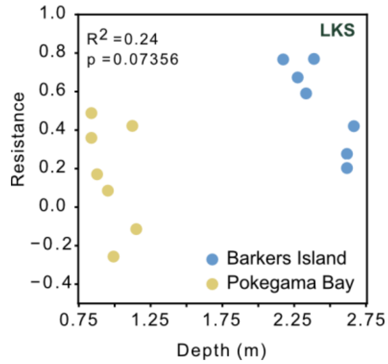

Fig. S12. Resistance versus depth relationship at Lake Superior NERR (LKS) with Oliver Bridge and Blatnik Bridge omitted due to positioning of the sondes within the water column (see Table S2).

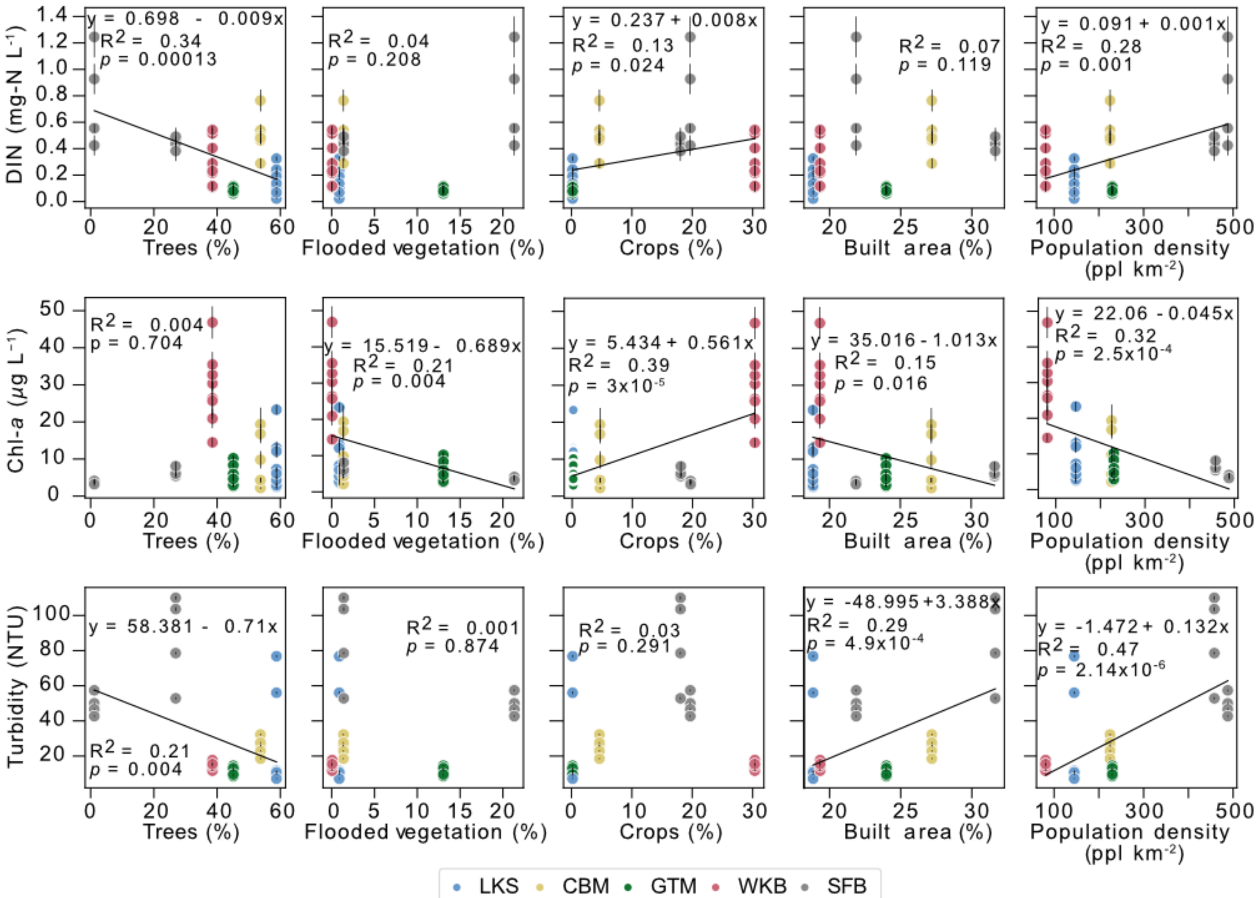

Fig. S13. Relationships of dissolved inorganic nitrogen (DIN), chlorophyll-*a* (Chl-*a*), and turbidity to land use/land cover and population density across estuaries. Estuary abbreviations: Lake Superior (LKS) NERR, Chesapeake Bay, Maryland (CBM) NERR, Guana Tolomato Matanzas (GTM) NERR, Weeks Bay (WKB) NERR, and San Francisco Bay (SFB) NERR. Regressions for significant relationships (p-value < 0.05) are shown in black lines. All relationships use annual means for physicochemical factors calculated for wet and dry years separately and land use/land cover characteristics adjoined to monitoring locations at each estuary.